scientific reports

Check for updates

OPEN

Experimental study on mechanical performance and microstructural characterization of optimized sisal fiber reinforced polyester composites

G. Sathishkumar[1], A. Uma Devi[2], M. Prem Kumar Reddy[3], Vishvanath N. Kanthe[4], D. Palaniswamy[5], P. R. Kalyana Chakravarthy[6], M. Dubey[7], Himadri Majumder[8] & Ashish Kumar Srivastava[9]✉

This study investigates the mechanical, dynamic, and thermal behavior of sisal fiber–reinforced polyester composites. Specimens were fabricated using manual hand layup with randomly distributed 20 mm sisal fibers at weight fractions of 5%, 10%, 15%, and 20%. Mechanical tests (tensile, flexural, impact, double shear, and compressive), free vibration analysis, damping evaluation, thermal characterization, and SEM imaging were performed. Results show that increasing fiber content enhanced most mechanical properties, natural frequency, and storage modulus, although peak damping values (tan δ) decreased with higher fiber loading. The highest impact strength (16 J) and compressive strength (52.4 MPa) were obtained at 20% fiber, while the most balanced overall performance was achieved at 15%, yielding maximum tensile strength of 17.44 MPa, flexural strength of 52.65 MPa, and shear strength of 77.97 MPa. Free vibration tests recorded a frequency of 67.38 Hz with a damping ratio of 0.059, and dynamic mechanical analysis reported a storage modulus up to 7.5 GPa. Thermal stability was maintained up to 300 °C, with rapid degradation above 400 °C and heat flux peaks at 600 °C. SEM analysis confirmed that fiber distribution and orientation strongly influenced composite performance. Overall, 15% sisal fiber content was identified as optimal for structural applications requiring balanced strength, dynamic behavior, and thermal stability.

Keywords Damping factor, FVT, Mechanical properties, Natural fiber, Polyester resin

Natural fiber composites present considerable advantages in comparison to synthetic fiber composites across a multitude of applications. The principal benefits include diminished costs, improved strength-to-weight ratios, and enhanced ecological sustainability[1–3]. The amalgamation of fibers derived from botanical sources with synthetic polymer matrices has exhibited remarkable efficacy, resulting in extensive industrial implementation. These composite materials leverage the intrinsic properties of natural fibers such as tensile strength, compressive resistance, impact energy absorption, and flexural behavior—making them viable alternatives for applications that prioritize resource efficiency[4–6].

The comprehension of the ramifications associated with vibrational phenomena is essential for the proficient development and implementation of composite materials. The analysis of vibrational behavior and damping

[1]Department of Mechanical Engineering, Vels Institute of Science, Technology & Advanced Studies, Chennai, Tamil Nadu 600117, India. [2]Department of Chemistry, St.Joseph's College of Engineering, OMR, Chennai, Tamil Nadu 600119, India. [3]Department of Mechanical Engineering, Aditya University, Surampalem, Andhra Pradesh 533437, India. [4]Department of Civil Engineering, Guru Gobind Singh College of Engineering and Research Center, Nashik, Maharashtra 422009, India. [5]Department of Mechanical Engineering, Adithya Institute of Technology, Coimbatore 641107, Tamil Nadu, India. [6]Department of Civil Engineering, Vels Institute of Science, Technology & Advanced Studies, Chennai, Tamil Nadu 600117, India. [7]Department of Mechanical Engineering, Bhilai Institute of Technology, Durg, Chhattisgarh 491001, India. [8]Department of Mechanical Engineering, G H Raisoni College of Engineering & Management, Pune, Maharashtra 412207, India. [9]Department of Mechanical Engineering, Manipal University Jaipur, Jaipur, Rajasthan 303007, India. ✉email: ashishkumar.srivastava@jaipur.manipal.edu

characteristics serves as a foundational method for investigating the mechanical properties of polymer composites; however, the damping mechanisms intrinsic to these composites exhibit marked distinctions from those identified in conventional polymers[7,8]. In contrast to homopolymer materials, fiber-reinforced composites possess intricate internal architectures that substantially influence their mechanical attributes. The efficacy of damping within these composites is contingent upon multiple factors, including the ratio of fillers, the quality of the interfaces, the orientation of applied stresses, and the degree of polymer plasticization. The aforementioned materials dissipate vibrational energy through various mechanisms, including the viscoelastic properties of both the matrix and the fibers, frictional losses at the matrix–fiber interfaces, energy dissipation caused by crack propagation and impact-induced delamination, as well as viscoelastic and thermoelastic damping phenomena[9–11].

The duration necessary for curing within the hand lay-up technique is contingent upon the specific polymer employed, with epoxy-based composites generally necessitating a temporal duration of 24 to 48 h when maintained under ambient thermal conditions. Although this technique is particularly advantageous for thermosetting polymer composites and requires a relatively modest capital investment, it is not without its limitations, which include protracted production rates and challenges in attaining elevated fiber volume fractions[12–14]. Notwithstanding these limitations, the hand lay-up method is widely adopted across various industries, including aerospace, automotive, marine, and construction, thereby enabling the application of a broad spectrum of composite materials[15].

Composite materials augmented with fillers exhibit intricate internal architectures that profoundly influence their functional efficacy. The effectiveness of their vibration attenuation is contingent upon a myriad of determinants, which include the volumetric proportion of reinforcement, the integrity of interfacial adhesion, the degree of polymer plasticization, and the orientation of applied mechanical loads[16–19]. These fiber-reinforced composites dissipate energy through a diverse range of mechanisms: the viscoelastic characteristics of both the matrix and the reinforcing fibers, frictional forces arising from the relative movement at the matrix-fiber interface, energy dissipation at sites of defects and regions experiencing impact-induced delamination, as well as the synergistic contributions of visco-plastic and thermoelastic damping phenomena[20–23].

Natural fibers from agricultural residues and biomass are gaining importance in sustainable composite manufacturing due to their renewability, biodegradability, low density, and high specific strength. Their properties depend on factors such as chemical composition, aspect ratio, and microfibril orientation, while moisture uptake and surface impurities often weaken fiber–matrix adhesion. Surface treatments, including alkali, silane, and hybrid methods, reduce hydrophilicity and improve interfacial bonding, resulting in enhanced mechanical performance and stability. Studies on fibers such as asparagus bean stem, *Ficus macrocarpa* bark, and *Mimosa pudica* report improvements in tensile strength and durability, supporting their use in additive manufacturing, automotive, construction, packaging, and lightweight structural applications as sustainable alternatives to synthetic reinforcements[24–26].

Recent research indicates that the properties of PLA composites can be significantly improved through the incorporation of various natural fibers and fillers, in conjunction with treatment techniques such as silane modification, to enhance mechanical strength, rigidity, thermal stability, and printability. Hybrid fiber systems, exemplified by Nona/Soy–PLA, provide a harmonious blend of distinct mechanical advantages, facilitating customized performance tailored to particular applications. Through the modulation of fiber type, surface treatment, and hybridization strategies, PLA filaments can attain superior thermo-mechanical characteristics, stability, biodegradability, and aesthetic qualities, thereby positioning them as a versatile and sustainable option for sophisticated additive manufacturing[27,28].

Natural fiber–reinforced PLA filaments combine sustainability and low weight with the potential for structural applications, but they face several processing and performance challenges. Both PLA and natural fibers are moisture-sensitive, and inadequate drying can degrade PLA, cause porosity, surface defects, and weaken printed parts; hence, pre-drying at 50–60 °C and sealed storage with desiccants are essential for quality control. Fiber variability in size and length affects filament uniformity, nozzle flow, and printer wear, while weak bonding with hydrophobic PLA often requires surface treatments or compatibilizers to improve adhesion. Thermal degradation above 200–230 °C further restricts processing with high-performance polymers, and printed parts frequently exhibit anisotropic strength, reduced durability, and lower impact resistance compared to neat PLA. Despite these issues, natural fiber composites are gaining attention in advanced fields such as ballistic protection[29], where their light weight, mechanical performance, and sustainability make them promising alternatives to synthetic reinforcements in defense and aerospace applications.

The investigation is centered on the formulation of composite materials utilizing natural sisal fibers for the fabrication of automotive dashboards. The study scrutinizes an array of natural fibers alongside optimization methodologies to augment mechanical performance, while concurrently exploring manufacturing techniques that transcend conventional hand layup approaches. Critical factors under consideration encompass aesthetic attributes, resistance to scratching, ultraviolet protection, and environmental sustainability, evaluated through comprehensive life cycle assessments[30,31]. The research endeavors to augment mechanical properties, including tensile, flexural, impact, and compressive strengths, whilst also assessing dynamic mechanical behavior under varying conditions. The study employs free vibration theory (FVT), thermogravimetric analysis (TGA), and scanning electron microscopy (SEM) to investigate fiber-resin interfaces and analyze different fiber orientations and thermal insulation properties, concentrating on optimal interior comfort, industrial scalability, and the potential for mass production[32,33].

Fig. 1. Sisal fiber.

Properties	Sisal
Density(g/cm^3)	1.33–1.45
Tensile strength	510–700
Young's modulus(GPa)	9–38
Moisture absorption %	11
Elongation at break (%)	2.2–2.9

Table 1. Mechanical properties of sisal fibers.

Materials and methods

Polyester resin

Polyester resins represent the most economically viable alternative for manufacturers producing fiberglass-reinforced plastic (FRP) vessels using molds. While being markedly more affordable than vinyl esters and epoxies, polyester resins exhibit several limitations: they demonstrate inadequate adhesion, high water permeability, and significant volumetric contraction during the curing process, and emit elevated concentrations of volatile organic compounds (VOCs)[34]. Furthermore, their applicability is restricted exclusively to fiberglass, thereby excluding other types of reinforcing fibers. Polyester resins are optimally utilized in straightforward applications where weight considerations are not paramount and substantial structural integrity is not requisite. Their efficacy is particularly pronounced in the fabrication of basic fiberglass components, which can be produced in a single operational step without the need for bonding, especially in scenarios where precise geometrical configurations are not crucial, exposure to moisture is not problematic, and adequate ventilation is ensured[35,36].

Sisal fibre

Natural fibers derived from renewable resources are increasingly recognized as viable alternatives to synthetic fibers, such as glass and carbon, for reinforcing polymer composites. sisal fiber is particularly notable for its efficacy, which is attributed to its high cellulose content and numerous practical advantages. These advantages encompass extensive availability, low density, cost-effectiveness, and robust physical and mechanical properties, thereby establishing it as one of the most prevalently utilized natural reinforcement materials, as illustrated in Fig. 1; Table 1[37].

Hand lay-up process

The hand lay-up technique represents the most basic approach for fabricating composite materials, requiring only a minimal array of equipment. This methodology entails the strategic placement of reinforcement materials, such as jute fibers, within a mold, followed by the application of a release agent and, subsequently, the pouring and distribution of thermosetting resin. A series of layers is accumulated, with the expulsion of air bubbles, and the composite undergoes a curing process before extraction from the mold[38–40]. Although this method is economically viable for limited production runs of items such as aircraft components, automotive parts, and marine hulls, it is constrained by a significant limitation: it cannot attain elevated ratios of reinforcement materials to resin, as illustrated in Fig. 2; Table 2.

The study conducted a thorough examination of sisal fibers (Fig. 3) using dynamic mechanical analysis, scanning electron microscopy, and mechanical property tests. Details of laminate construction were documented, including fiber orientation, weight distribution, and stacking sequence. Testing was conducted in accordance

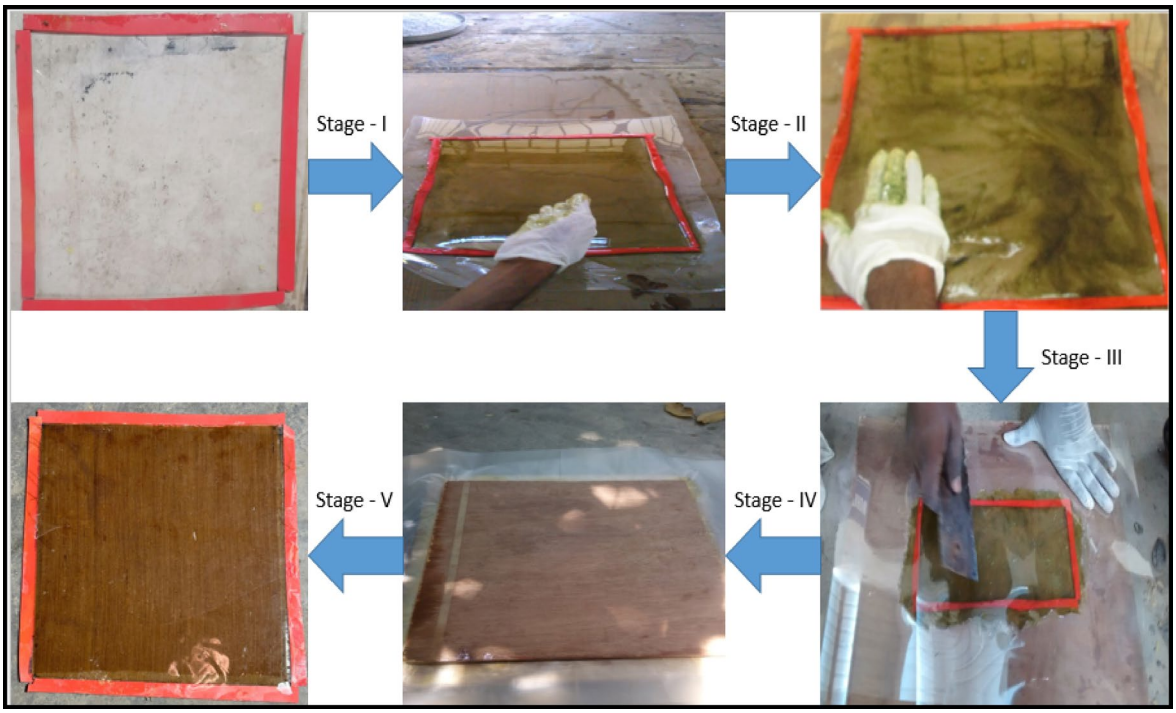

Fig. 2. Hand lay process.

Sample	Sisal Mass
Sample:1	17.95 g
Sample: 2	35.91 g
Sample: 3	53.86 g
Sample: 4	71.82 g

Table 2. Volumes and mass calculation of sisal fiber.

with ASTM standards for multiple properties, including tensile, flexural, compressive strength, shear strength, impact resistance, thermal behavior, natural frequency, and microscopic structure.

Results and discussion

Mechanical properties for sisal fiber reinforced composite materials

The research endeavor concentrated on assessing the extent to which various proportions of sisal fiber affect the mechanical characteristics of a composite material (Table 3). Mechanical tests (tensile, flexural, impact, double shear, and compressive) were conducted on three specimens for each test condition. At a fiber content of 5%, the composite demonstrated relatively moderate performance, exhibiting an impact strength of 1.33 Joules, a tensile strength of 4.39 MPa, a flexural strength of 47.17 MPa, a shear strength of 46.48 MPa, and a compressive strength of 14.46 MPa. These measurements imply that the reinforcing impact of sisal fibers at this concentration is minimal. Conversely, when the sisal content was augmented to 10%, a significant enhancement was observed across all evaluated properties. The impact strength escalated to 4 Joules, the tensile strength increased considerably to 16.72 MPa, the flexural strength attained 48.9 MPa, the shear strength rose to 49.38 MPa, and the compressive strength improved to 25.85 MPa. This trend persisted at a sisal content of 15%, where the composite exhibited even superior mechanical performance: impact strength reached 6.66 Joules, tensile strength rose to 17.44 MPa, flexural strength increased to 52.65 MPa, shear strength peaked at 77.97 MPa, and compressive strength advanced to 42.54 MPa. These findings suggest that a sisal fiber content of 15% may represent an optimal equilibrium for reinforcing the composite. However, at a fiber content of 20%, the findings became increasingly complex. While the impact strength achieved its zenith at 16 Joules and compressive strength reached a maximum of 52.4 MPa, other properties exhibited a decline. The tensile strength diminished to 11.88 MPa, the flexural strength decreased to 39.35 MPa, and the shear strength fell to 55.3 MPa. This indicates that an excessive fiber content may precipitate complications such as inadequate dispersion, fiber agglomeration, or compromised matrix bonding, ultimately undermining certain mechanical attributes despite improvements in others.

Fig. 3. Testing samples.

S. no.	Mechanical properties	Weight% of the fiber			
		Sisal 5%	Sisal 10%	Sisal 15%	Sisal 20%
1	Impact values, joules	1.33	4	6.66	16
2	Tensile strength, MPa	4.39	16.72	17.44	11.88
3	Flexural strength, MPa	47.17	48.9	52.65	39.35
4	Shear strength, MPa	46.48	49.38	77.97	55.3
5	Compressive strength, MPa	14.46	25.85	42.54	52.4

Table 3. Mechanical properties of sisal fiber-reinforced composite materials.

S. no	Mechanical properties	Sisal 5%	Sisal 10%	Sisal 15%	Sisal 20%
1	Impact values (J)	1.33 ± 0.15	4.00 ± 0.35	6.66 ± 0.50	16.00 ± 1.80
2	Tensile strength (MPa)	4.39 ± 0.40	16.72 ± 0.95	17.44 ± 0.27	11.88 ± 1.65
3	Flexural strength (MPa)	47.17 ± 1.80	48.90 ± 1.20	52.65 ± 0.90	39.35 ± 2.50
4	Shear strength (MPa)	46.48 ± 2.10	49.38 ± 1.80	77.97 ± 1.50	55.30 ± 3.80
5	Compressive strength (MPa)	14.46 ± 0.90	25.85 ± 1.40	42.54 ± 1.10	52.40 ± 2.20

Table 4. Mechanical properties of sisal fiber composite materials with standard deviation.

The mechanical properties of the sisal fiber-reinforced polyester composites, presented as mean ± standard deviation ($n = 3$) in Table 4, it demonstrates the influence of fiber loading on performance and the critical consistency of the results. The optimally performing 15% fiber composite exhibited the highest mean values in tensile, flexural, and shear strength, coupled with the lowest standard deviations for these properties. The 20% of fiber composite, while superior in impact resistance, showed significantly larger standard deviations in tensile and shear strength, supporting the closes to the fiber agglomeration introduces variability and defects, thereby compromising the reliability of its mechanical performance despite a high average value in compression. The low

standard deviations across the lower fiber content composites further validate the experimental methodology and highlight 15% as the most robust and dependable formulation.

The illustration in Fig. 4 depicts the results of tensile testing conducted on sisal fiber composites, which indicates a distinct trend. As the proportion of sisal fiber increased from 5% to 15%, there was a consistent enhancement in tensile strength, ultimately attaining a maximum value of 17.44 MPa at a fiber content of 15%. Nevertheless, an increase in fiber content to 20% resulted in a pronounced reduction in tensile strength. This observation underscores the critical significance of employing optimal fiber content, specifically 15% to realize superior tensile properties in sisal fiber composites.

The increase in tensile strength shows that an optimum is reached at 15% before decreasing. The strength rises sharply from 4.39 MPa (5%) to 17.44 MPa (15%), then falls to 11.88 MPa (20%). This trend is highly dependent on the efficiency of stress transfer from the matrix to the fibers, which requires excellent bonding. The increase up to 15% shows the fibers are effectively sharing the tensile load. The subsequent decrease at 20% is a classic sign of fiber agglomeration, where excessive fibers can no longer be properly wetted by the resin, leading to poor adhesion, voids, and stress concentrations that cause premature failure.

The graphical representation in Fig. 5 illustrates that the flexural tests indicate the incorporation of sisal fiber significantly enhances the composite's resistance to bending, with the most favorable outcomes observed at a fiber content of 15%, where the flexural strength reaches a maximum of 52.65 MPa. Conversely, an increase in fiber content to 20% resulted in a significant reduction in bending strength, with a decrease of 13.3 MPa. This observation highlights the importance of meticulous regulation of fiber content, particularly at the 15% level, for achieving optimal bending characteristics in sisal fiber composites.

The increase in flexural strength shows an optimum at 15% before a significant decrease. It rises modestly from 47.17 MPa to 52.65 MPa at 15%, then drops to 39.35 MPa at 20%. Flexural strength measures resistance to bending, which induces both tensile and compressive stresses. The initial increase is due to the fibers effectively resisting these stresses. The sharp decline at 20% is again caused by insufficient matrix material to hold the fibers together and transfer stress effectively, leading to premature failure under the combined loads.

The graphical representation, designated as Fig. 6, illustrates that the results of impact testing demonstrate a substantial enhancement in the impact resistance of the composite material with an increase in sisal fiber content from 5% to 20%. The peak impact strength was recorded at an impressive 16 Joules when the fiber content was 20%, which is twelve times greater than that observed in composites containing 5% fiber. This consistent enhancement suggests that elevated levels of sisal fiber are crucial to the development of composites that exhibit superior impact energy absorption capabilities.

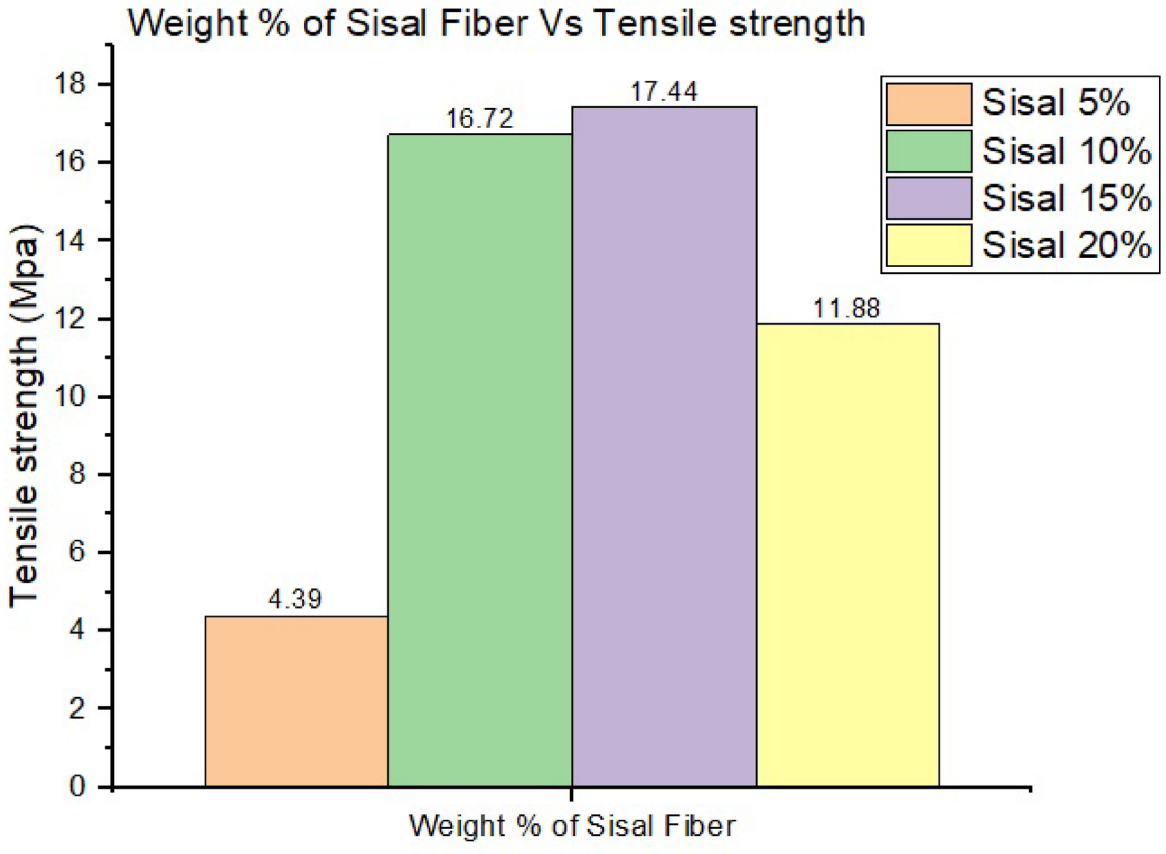

Fig. 4. Wt. % of sisal fiber vs. ultimate strength.

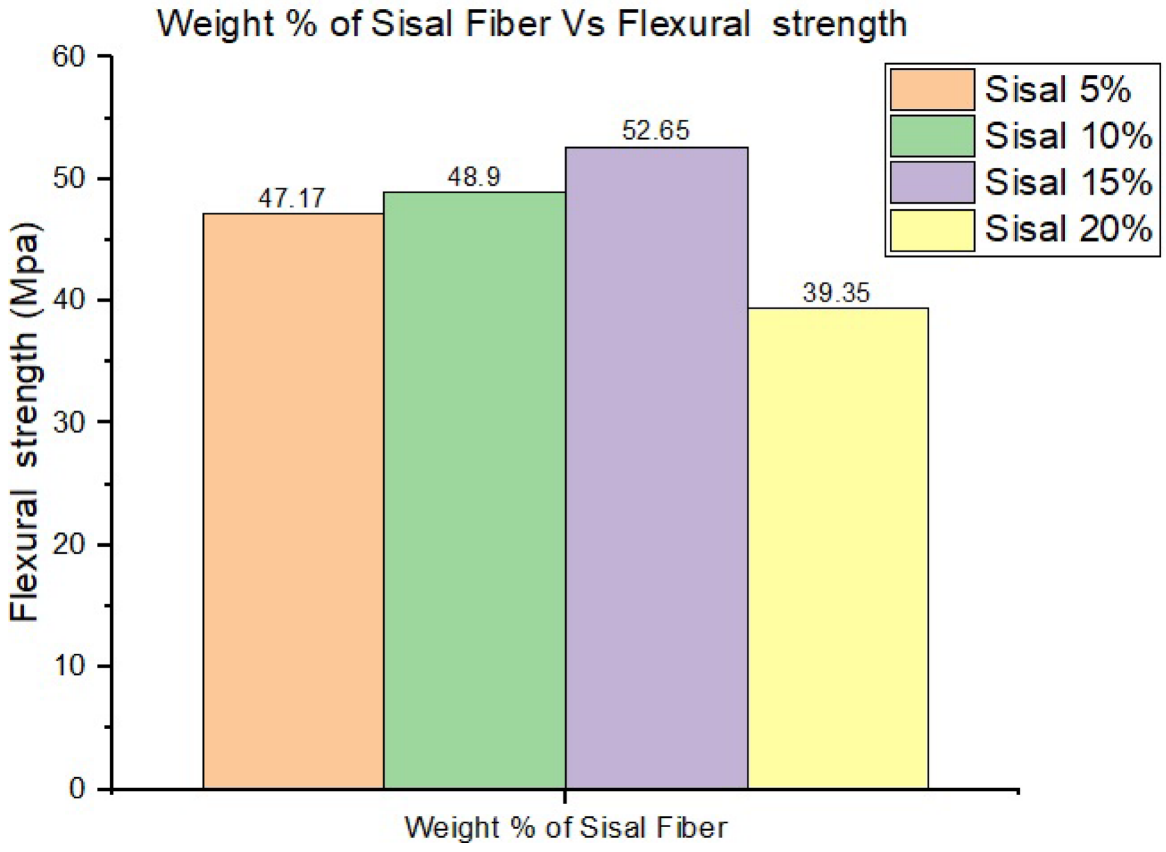

Fig. 5. Wt. % of sisal fiber vs. flexural strength.

Impact strength exhibits a steady and sharp increase from 1.33 J at 5% fiber to 16 J at 20% fiber, this consistent upward trend is due to the role of fibers in absorbing energy. As fiber content increases, more energy is required to debond the fibers from the matrix and pull them out, which is a primary energy-absorbing mechanism in composites. Higher fiber content also creates a more complex network that forces cracks to take a longer, more tortuous path, thereby absorbing more energy before causing failure. This indicates that toughness and damage tolerance are maximized at the highest fiber loading of 20%.

The graphical representation labeled as Fig. 7 indicates that empirical investigations have demonstrated a robust correlation between the percentage of sisal fiber incorporated and the resultant compressive strength of the composite material. As the fiber content was augmented from 5% to 20%, a consistent enhancement in compressive strength was observed, culminating in a peak value of 52.4 MPa at the 20% fiber content level. The most pronounced enhancement was noted within the interval of 10% to 15% fiber content, suggesting that this specific range is particularly efficacious in augmenting the composite's capacity to withstand compressive forces.

In compressive strength analysis shows that a steady and consistent increase from 14.46 MPa at 5% to 52.4 MPa at 20%. Unlike tensile strength, compressive strength benefits from the pure physical presence of stiff fibers that resist buckling and crushing. The mechanism here is more reliant on fiber loading than perfect interfacial bonding. The continuous increase suggests that the fibers act as reinforcing pillars that support the matrix, and this positive effect outweighs the negative impact of any minor agglomeration or poor bonding at 20% for this specific failure mode.

The graphical representation in Fig. 8 indicates that double shear testing has demonstrated a significant correlation between sisal fiber content and the shear strength of the composite material. Specifically, as the fiber content was incrementally increased from 5% to 15%, a notable enhancement in shear strength of 67.8% was observed, culminating in a maximum value of 77.97 MPa. Conversely, an additional increase in fiber content to 20% resulted in a reduction of shear strength. This observation suggests that a fiber content of 15% constitutes the optimal threshold for enhancing the shear resistance in sisal fiber-reinforced composites.

The shear strength analysis shows a dramatic increase to an optimum at 15% before decreasing. It makes a significant jump to 77.97 MPa at 15%, then falls to 55.3 MPa at 20%. Interlaminar shear strength is a critical indicator of the quality of the fiber-matrix interfacial bond. The peak at 15% signifies the optimal loading for interfacial adhesion, where the matrix fully wets the fibers to create a strong bond. The severe drop at 20% confirms that fiber agglomeration and poor wetting create weak points and voids at the interface, drastically reducing the material's resistance to shearing forces.

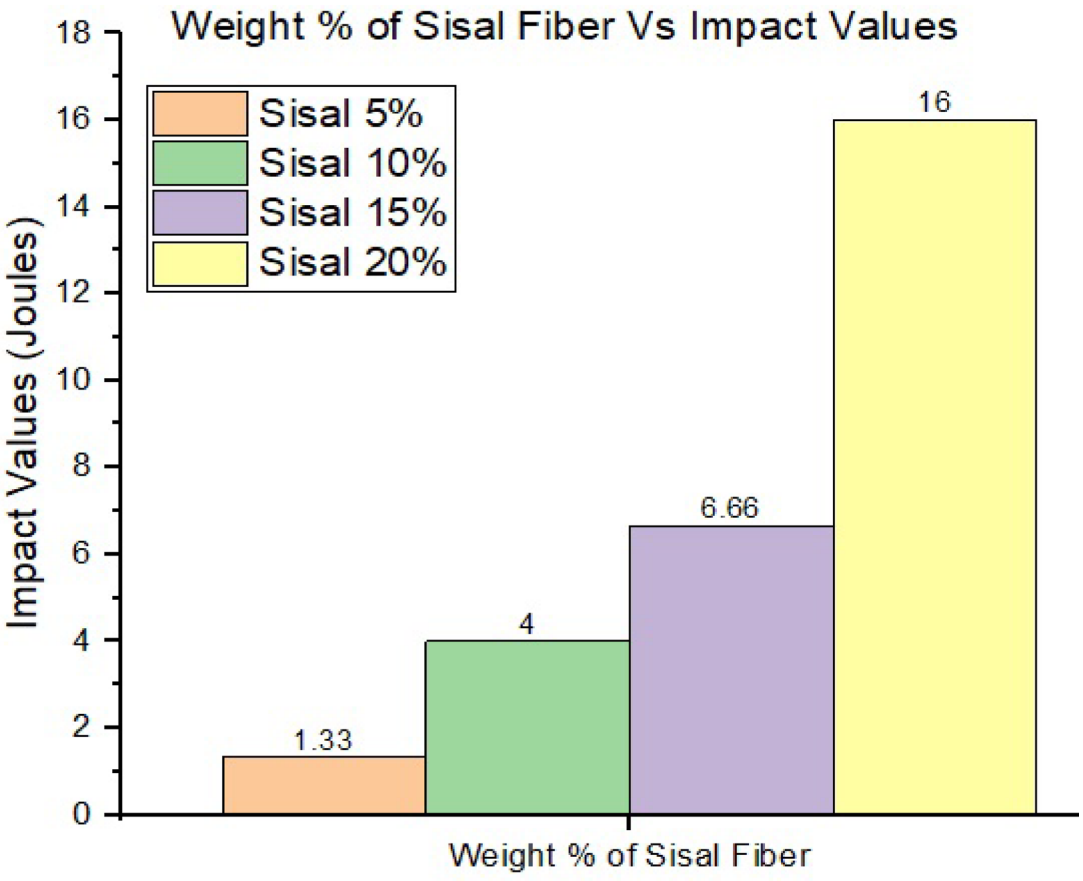

Fig. 6. Wt. % of sisal fiber vs. impact strength.

FVT - Free vibration analysis for sisal fiber

Natural frequency

Free vibration experiments were performed on cantilever beams by instigating vibrations and documenting acceleration data. The natural frequencies were ascertained via Fourier analysis, whereas measurements of acceleration decay yielded damping ratios. The experimentation encompassed composites comprising 5–20% sisal fiber by weight, with Figs. 9a–d illustrating the variation of natural frequency and vibration amplitude in relation to fiber content.

Free vibration and temporal history analyses were conducted on polyester composites enhanced with varying weight proportions of sisal fiber, specifically 5 wt%, 10 wt%, 15 wt%, and 20 wt%. The principal aim of these analyses was to evaluate the dynamic behavior of the composites and determine the degree to which fiber content influences their vibrational characteristics. The natural frequencies corresponding to each composite configuration were calculated utilizing the methodology outlined in the relevant section of the study. The results are visually depicted in Fig. 9a–d, which collectively illustrate the progression of natural frequency across different fiber compositions. Each sub-figure not only highlights the frequency values but also integrates Frequency vs. Amplitude plots, thereby providing a clear representation of how the amplitude response varies with frequency for each composite type. These graphical representations yield substantial insights into the vibrational performance of the materials, suggesting that fluctuations in sisal fiber content exert a direct and measurable impact on the dynamic properties of the polyester matrix.

The graphical representation illustrated in Fig. 10 unequivocally delineates the influence of sisal fiber content on the natural frequencies of polyester composites subjected to free vibration analysis. As the concentration of sisal fiber increases, there is a corresponding rise in the natural frequency, which denotes an improvement in vibrational performance. Specifically, the foundational polyester composite incorporating 5% sisal fiber exhibited the lowest frequency of 27.63 Hz. Upon increasing the fiber content to 10%, the frequency ascended to 31.75 Hz, and at 15%, it reached a peak of 67.38 Hz, thereby demonstrating the highest vibrational efficacy among the samples examined. Notably, at 20% sisal fiber, the frequency diminished to 46 Hz, suggesting that exceeding a certain threshold may lead to a decrease in the benefits associated with fiber reinforcement due to occurrences such as fiber agglomeration or a compromised matrix integrity. In conclusion, the observed trend emphasizes that gradual increases in sisal fiber content, particularly up to 15%, can significantly enhance the dynamic characteristics of the composite, rendering it more suitable for applications requiring elevated natural frequencies and improved vibration resistance.

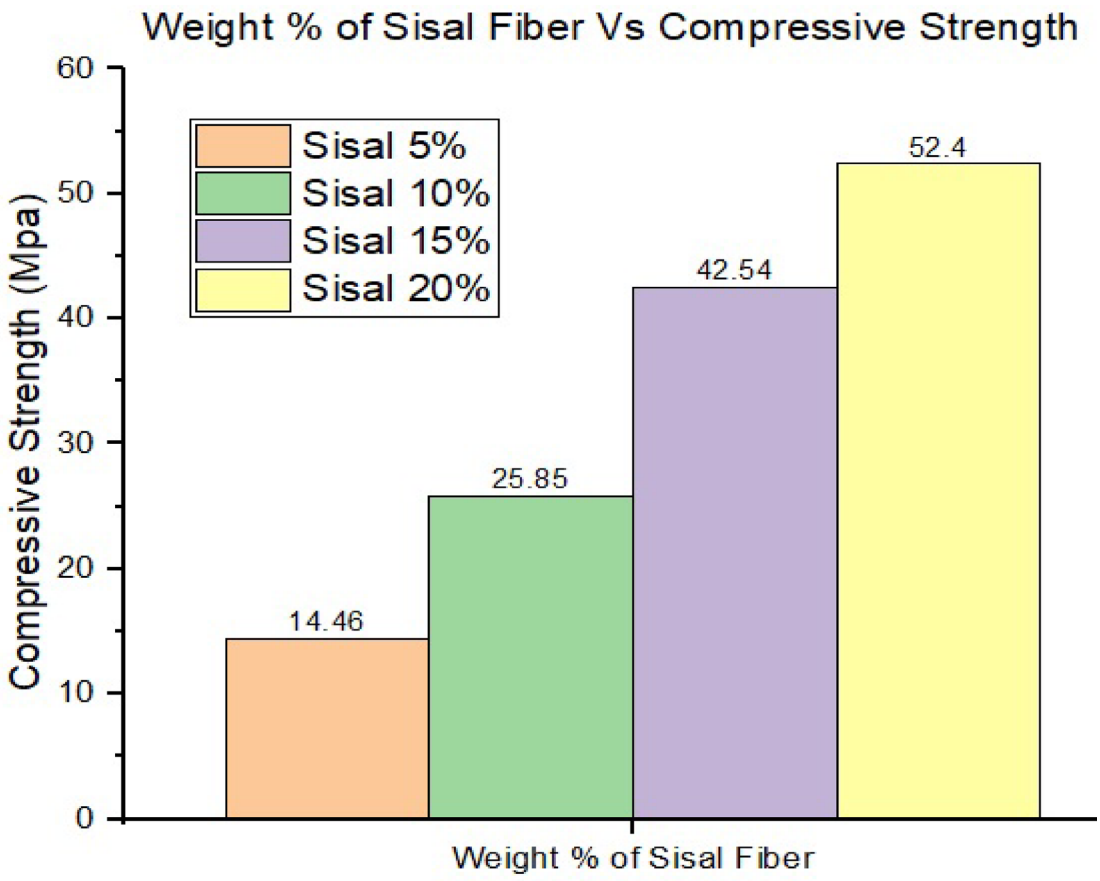

Fig. 7. Wt. % of sisal fiber vs. compressive strength.

Damping curve

Free vibration experiments were conducted on polyester composites incorporating 5–20% sisal fiber content. Graphical representations of acceleration in relation to time for each composite formulation are illustrated in Figs. 11a–d**.** The findings elucidate the influence of sisal fiber incorporation on the damping ratio in comparison to unaltered polyester. These empirical measurements are instrumental in elucidating the vibrational and damping characteristics of the materials.

Calculation for Damping Ratio.

Find out the Damping ratio of the material using logarithmic decrement Formula-1.

$$\ln\frac{x_1}{x_2} = \frac{2\pi\,\epsilon}{\sqrt{1-\epsilon^{\,2}}} \tag{1}$$

Where:

X_1 is i^{th} peak.

X_2 is the peak acceleration of the peak after i^{th} peak.

20Wt. % of sisal Fiber

$x_1 = 1.811$.

$x_2 = 1.396$.

These values are taken from the acceleration Vs time graph of pure polyester.

$$\ln\frac{1.811}{1.396} = \frac{2\pi\,\epsilon}{\sqrt{1-\epsilon^{\,2}}},\ \epsilon = 0.0369$$

The data presented in Fig. 12 illustrates that an increased proportion of sisal fiber within the polyester composite correlates with a progressive enhancement in the damping ratio. The reference polyester formulation containing 5% sisal fiber exhibits the lowest damping ratio recorded at 0.024, whereas the composition incorporating 15% sisal fiber attains the highest damping ratio of 0.059. This positive correlation suggests that the incorporation of a greater quantity of sisal fiber significantly augments the composite's capacity to mitigate vibrational energy.

It has been observed that the temporal span of decay experiences a reduction with the inclusion of sisal fiber, with the minimum duration of decay occurring at a concentration of 20wt. % within sisal fiber composite materials, as referenced in Table 5.

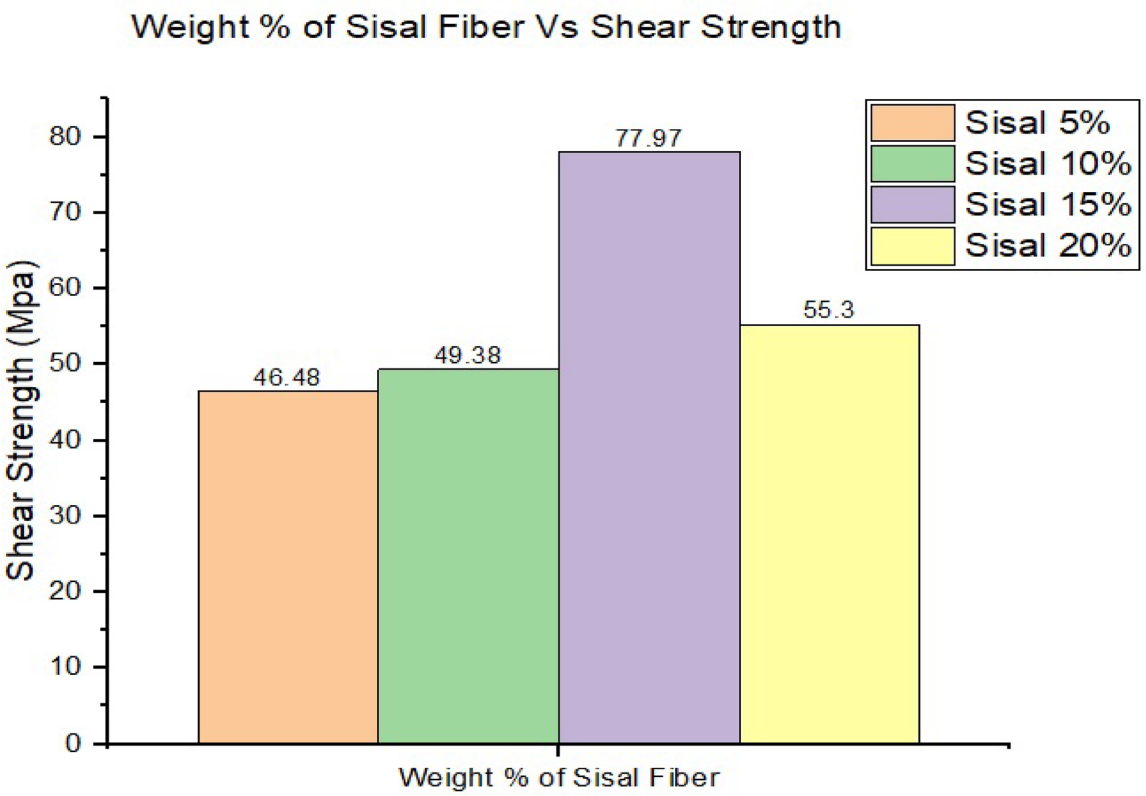

Fig. 8. Wt. % of sisal fiber vs. shear strength.

Dynamic mechanical analysis (DMA)

The test specimen exhibits dimensions of 40 mm in length, 10 mm in width, and 3 mm in thickness. The experimentation is performed across a thermal spectrum ranging from 25 °C to 180 °C, employing a heating velocity of 2 °C per minute[24–26]. The assessment of the material is conducted using bending tests configured in either a 3-point or dual cantilever arrangement, with operational frequencies set at 0.5, 1, 2, 5, and 10 Hz. DMA functions as a proficient technique for clarifying how the viscoelastic response of polymers is affected by variations in temperature, time, and frequency. The integration of sisal fibers has significantly enhanced the thermo-mechanical characteristics of the polyester composite. As the proportion of sisal fiber increased from 5% to 20%, a systematic enhancement was observed in both the storage modulus (which denotes stiffness) and the loss modulus (which reflects damping).Furthermore, the glass transition temperature exhibited an upward trend, concomitant with an increase in fiber content. At lower thermal conditions, the pronounced disparity between the storage and loss moduli suggested elastic, solid-like characteristics. In contrast, their convergence at elevated temperatures indicated a transition toward enhanced viscous damping behavior. These findings substantiate the assertion that incorporating sisal fibers significantly improves both the mechanical and thermal properties of the polyester composite, thereby rendering it suitable for a diverse range of applications, as illustrated in Figs. 13a–d.

The data illustrated in Fig. 14 indicates that both an elevated content of sisal fiber and an increase in testing frequencies contribute to an enhancement in the storage modulus of the polyester composite, thereby suggesting superior stiffness and energy storage capabilities. Composites comprising 15–20% sisal fiber achieved storage modulus values of up to 7.5 GPa, which is significantly higher than the 2–3 GPa range observed in composites containing only 5% sisal fiber. This evidence suggests that incorporating a higher proportion of sisal fiber, in conjunction with increased testing frequencies, enhances the mechanical properties of the composite.

The data presented in Fig. 15 illustrates that an escalation in the proportion of sisal fiber within the polyester composite markedly enhances its loss modulus, signifying a superior capacity for energy dissipation. Composites containing 15–20% sisal fiber exhibited loss modulus values approximately fourfold greater than those containing merely 5% sisal fiber. Nevertheless, an increase in testing frequencies resulted in a diminution of the loss modulus, implying that sisal-reinforced composites are more proficient in energy dissipation at lower frequencies.

Figure 16 indicates that the tan delta (damping) exhibits a decrement at elevated frequencies across all polyester-sisal compositions. The composite formulation incorporating 15% sisal fiber demonstrated minimal tan delta values, which signifies a reduction in damping characteristics, whereas the 5% sisal composition exhibited the maximal values. This observation suggests that incorporating 15% sisal content facilitates the optimal balance of damping properties within the composite material. The graphical representation in Fig. 17 indicates that, at an elevated temperature of 80 °C, an increase in the content of sisal fiber correlates with a reduction in tan delta (damping factor) values across all examined frequencies. The composite material incorporating 5% sisal fiber

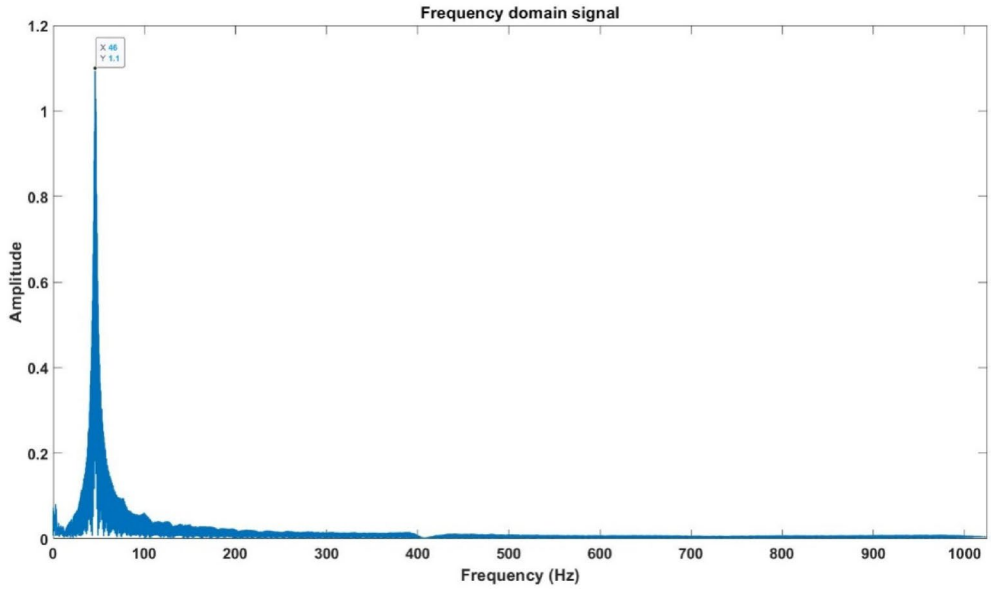

(a)

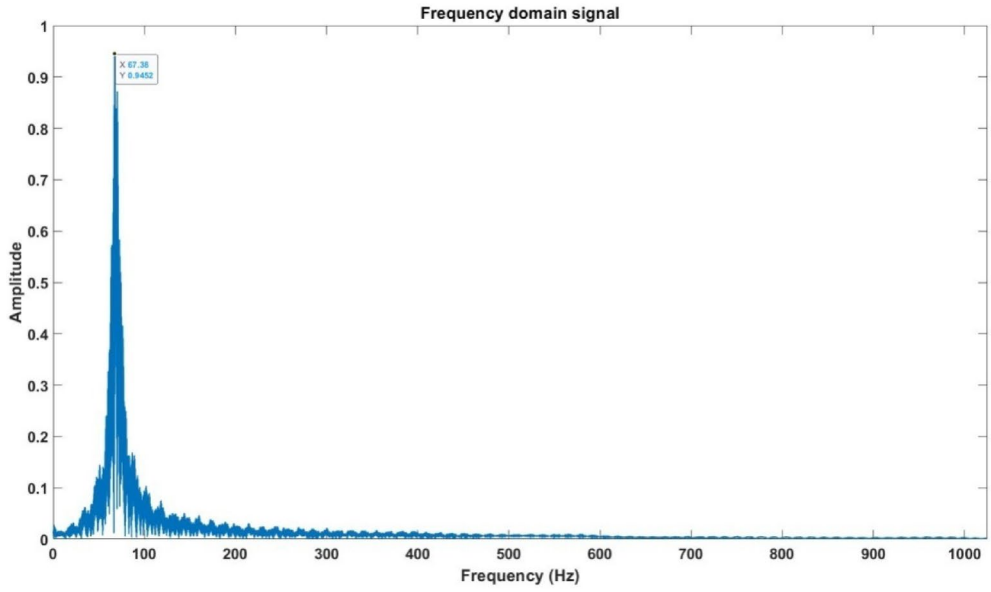

(b)

Fig. 9. (**a**) 5 Wt.% of sisal fiber Freq. (Hz) vs. Amp. (g); (**b**) 10 Wt.% of sisal fiber Freq. (Hz) vs. Amp. (g); (**c**) 15 Wt.% of sisal fiber Freq. (Hz) vs. Amp. (g); (**d**): 20 Wt. % of sisal fiber Freq. (Hz) vs. Amp. (g).

demonstrated the most substantial tan delta values, whereas the composition containing 20% sisal fiber revealed the least significant values.

TGA - thermal analysis

The simultaneous thermal analysis apparatus amalgamates differential scanning calorimetry (DSC) and thermogravimetric analysis (TGA) functionalities to enable a comprehensive characterization of materials through precise thermal regulation. Operating within a temperature spectrum extending from ambient conditions to 800 °C with a precision of ± 0.5 °C, the investigation employed dual identical thermal cycles conducted at a rate of 15 °C/min. This methodical heating protocol elucidated two predominant thermal phenomena: a pronounced mass reduction identified at 400 °C and significant thermal transitions occurring at 600 °C, as substantiated by congruent peaks in both heat flow and temperature differential analyses[27,28]. The

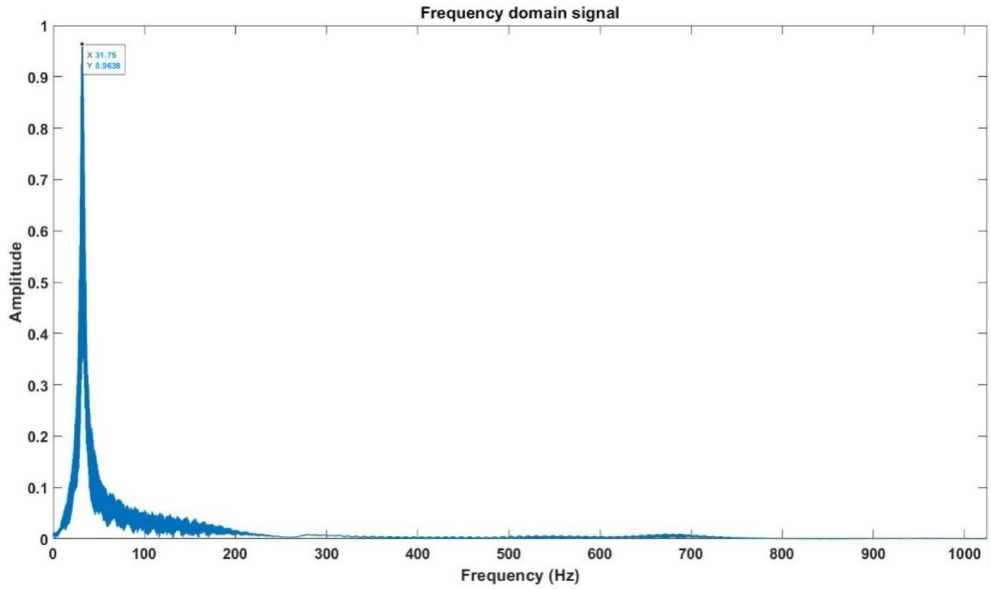

(c)

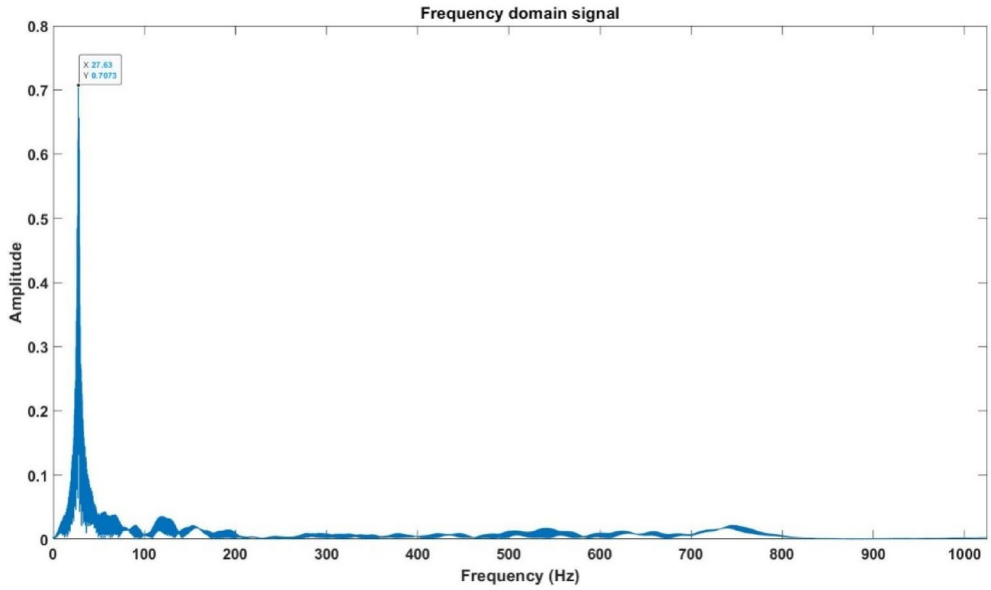

(d)

Fig. 9. (continued)

consistent heating rate, in conjunction with the dual-cycle approach, ensures enhanced reproducibility and reliability of data throughout the thermal characterization process.

In Fig. 18, the thermal analysis data represented as "PR" elucidates complex material behaviour within a temperature range extending from 0 to 800 °C. The graphical depiction concurrently evaluates three critical parameters: temperature differential, thermal flow, and mass percentage. Initially, the specimen retains a stable mass of approximately 100% until it reaches 300 °C, beyond which it undergoes a significant mass reduction, declining to nearly 0% by 400 °C. This remarkable decrease in mass suggests a substantial decomposition or degradation phenomenon. Concurrently with these changes, the normalized thermal flow initiates at −2 W/g and progressively decreases until it attains 400 °C, where it experiences a slight fluctuation before exhibiting a pronounced peak around 600 °C. The temperature differential demonstrates a similar trajectory, revealing an initial minor decline followed by a gradual increase, culminating in a sharp peak also near 600 °C, albeit of slightly lesser magnitude than the thermal flow peak. Subsequently, both parameters exhibit a steady decline as they approach the upper temperature threshold of 800 °C. The emergence of these peaks at 600 °C, occurring

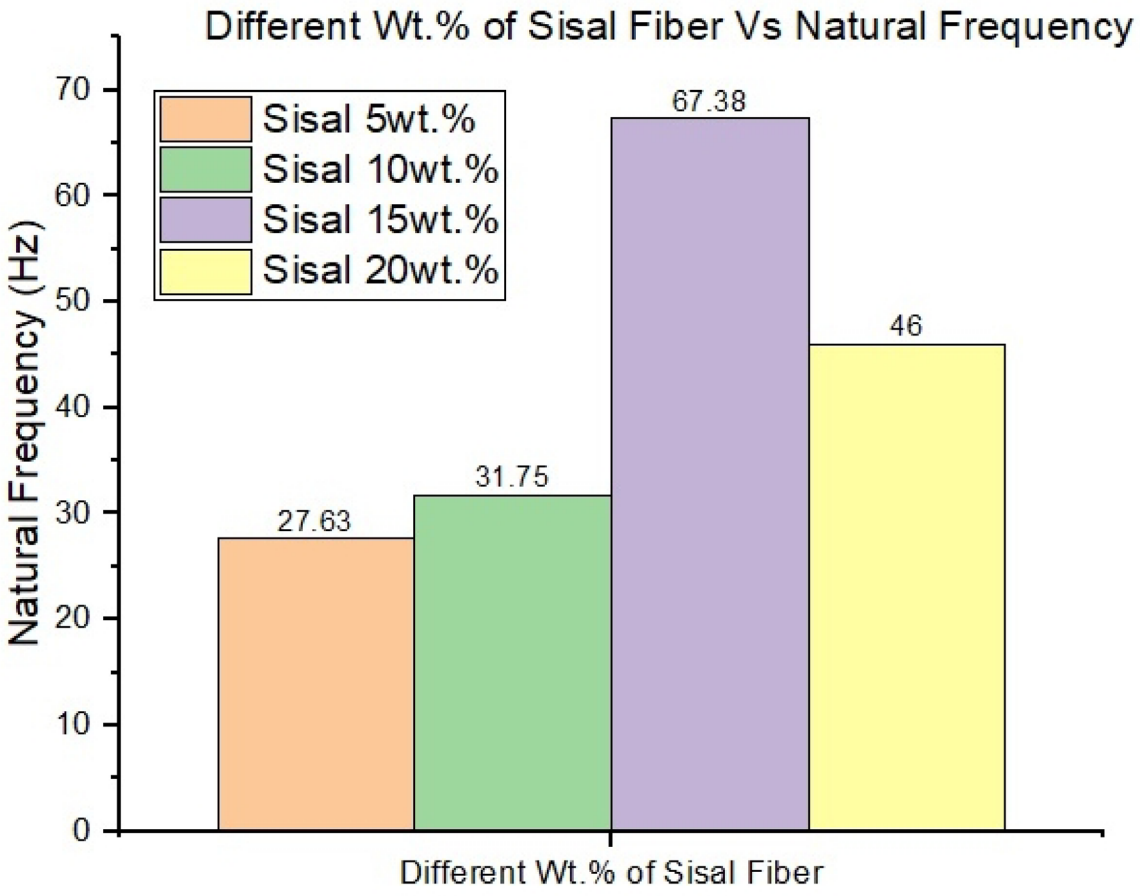

Fig. 10. Wt. % of sisal fiber vs. natural frequency.

after the considerable mass loss, signifies a significant thermal event, potentially indicative of a phase transition or crystallization in the residual material.

Scanning electron microscopy (SEM)

SEM represents a sophisticated methodology for the examination of surface morphology and material composition at elevated magnifications. This technique employs an electron beam, specialized optical systems, and detectors to generate intricate images through interactions with the surface of the sample[29]. The SEM analysis was conducted at METMECH Analytical Engineers, Ekkatuthangal, Chennai, Tamil Nadu, India. Adequate preparation of samples, encompassing processes such as cleaning and coating, is imperative for the effective execution of SEM imaging and elemental analysis through techniques such as Energy Dispersive Spectroscopy (EDS).

The adaptability of SEM renders it indispensable in the domains of materials science, nanotechnology, and biology, as it furnishes comprehensive insights into surface characteristics and compositional attributes. Figure 19 shows the 5% sisal composite SEM image; it shows the various failure mechanisms. The SEM image reveals gaps between sisal fibers and the polyester matrix, indicating poor interfacial adhesion. This defect occurs due to the incompatibility between hydrophilic sisal fibers and hydrophobic polyester resin, as well as insufficient wetting during processing. Weak bonding reduces load transfer efficiency, leading to premature failure under mechanical stress. Brittle fractures in the polyester resin appear as smooth; the cracks originate from stress concentrations around fiber ends or voids, propagating under load. The high resin content of 95% makes the matrix prone to brittle failure, reducing overall ductility. Optimizing curing conditions or incorporating toughening agents could mitigate this issue.

Figure 20 shows the 5% sisal composite SEM image; the fiber-matrix debonding shows the poor interfacial adhesion between fibers and matrix, evidenced by visible gaps. Fiber pull-out dominates the failure mode, with numerous cavities indicating fiber detachment rather than fracture. Brittle Matrix Cracking appears as sharp cracks in the polyester resin, while fiber fracture demonstrates fiber breakage under stress. The fiber fracture confirms some load transfer occurred, but the overall damage pattern suggests interfacial weakness is the primary failure origin, consistent with natural fiber composite behavior.

Figure 21 shows the 15% sisal composite SEM image; it reveals two defects in the sisal-polyester composite. Void formation appears as scattered dark pores, suggesting imperfect resin flow or moisture release during

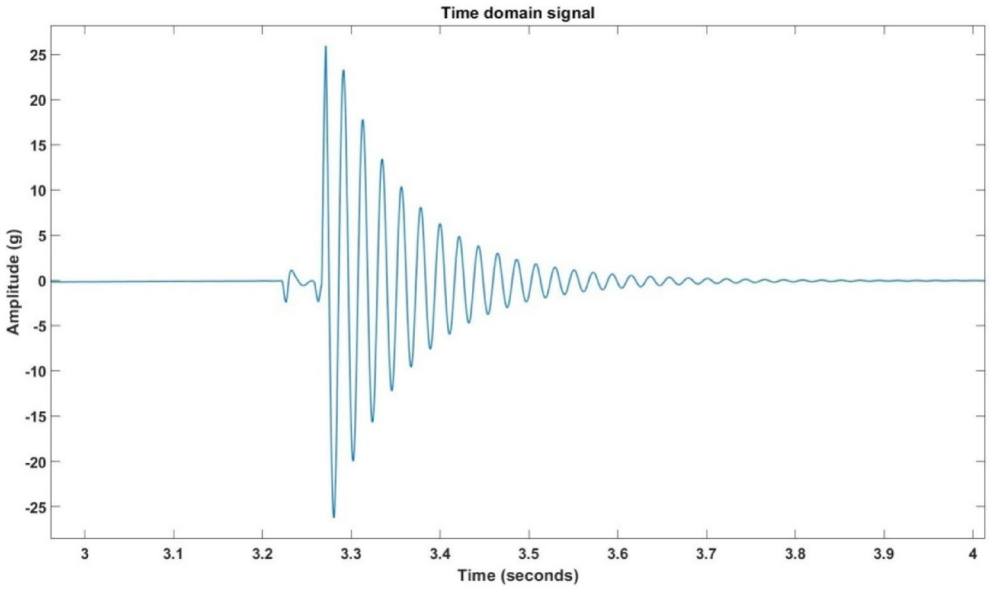

(a)

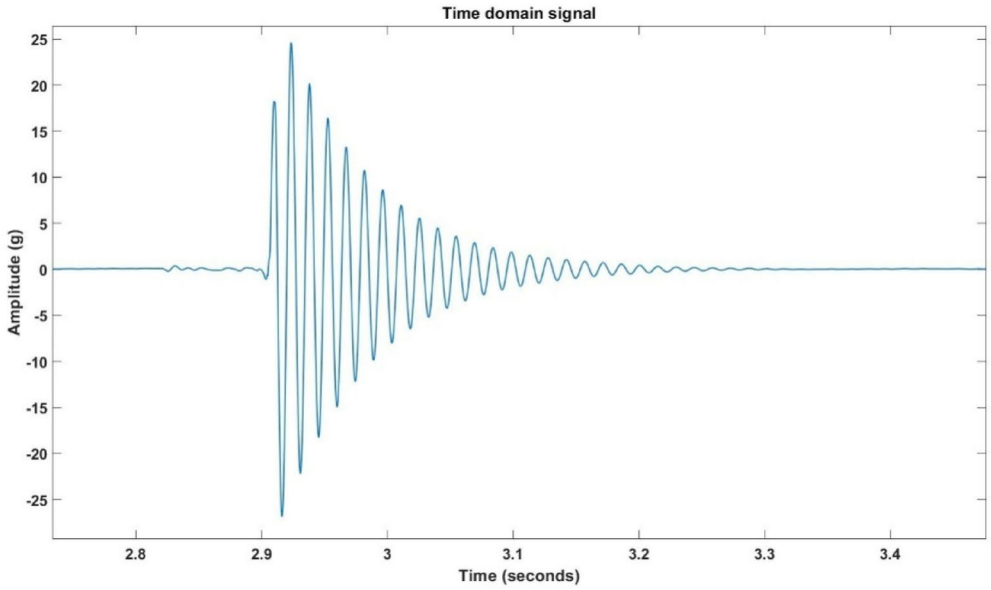

(b)

Fig. 11. (**a**) 5 Wt.% of sisal fiberTime vs. Amp.; (**b**) 10 Wt.% of sisal fiber vs. time vs. Amp.; (**c**) 15 Wt.% of sisal fiberTime vs. Amp.; (**d**) :20 Wt.% of sisal fiberTime vs. Amp.

processing, which compromises structural integrity by creating stress concentration sites. Fiber fracture displays cleanly broken fibers with fibrillated ends, indicating localized overloading and insufficient stress distribution.

Figure 22 shows the 20% sisal composite SEM image; the SEM image reveals three failure mechanisms in the composite. The void formation appears as irregular pores within the matrix, resulting from processing defects or moisture release, which act as stress concentrators during loading. Matrix Debonding is evident through distinct fiber-matrix separations, indicating weak interfacial bonding that compromises load transfer efficiency. Void formation initiates crack propagation, while matrix debonding accelerates it along fiber interfaces. The scanning electron microscopy (SEM) micrographs presented in this investigation elucidate how the distribution, orientation, and interfacial properties of fibers significantly influence the mechanical and dynamic characteristics of composites reinforced with sisal fibers.

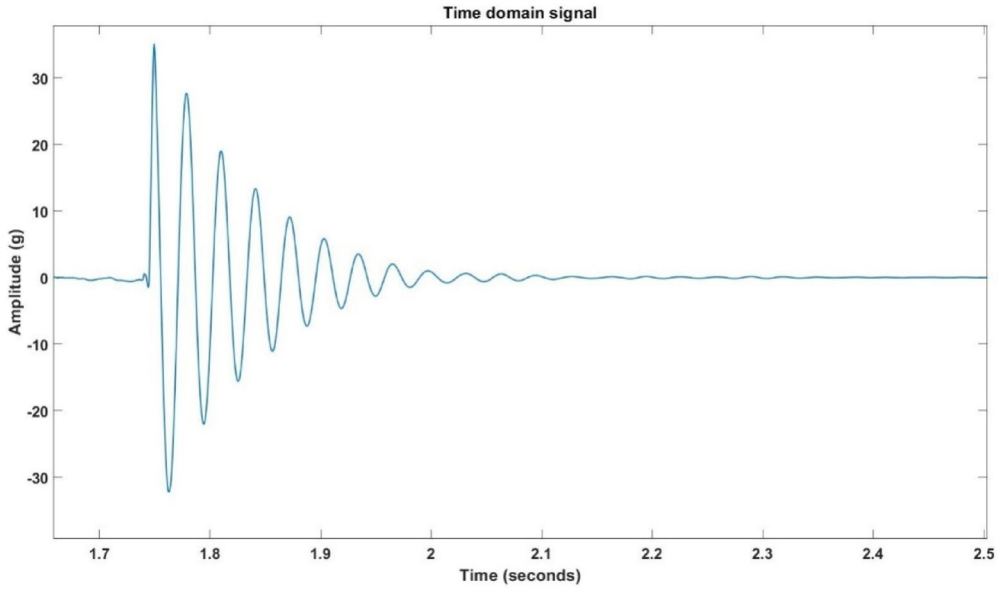

(c)

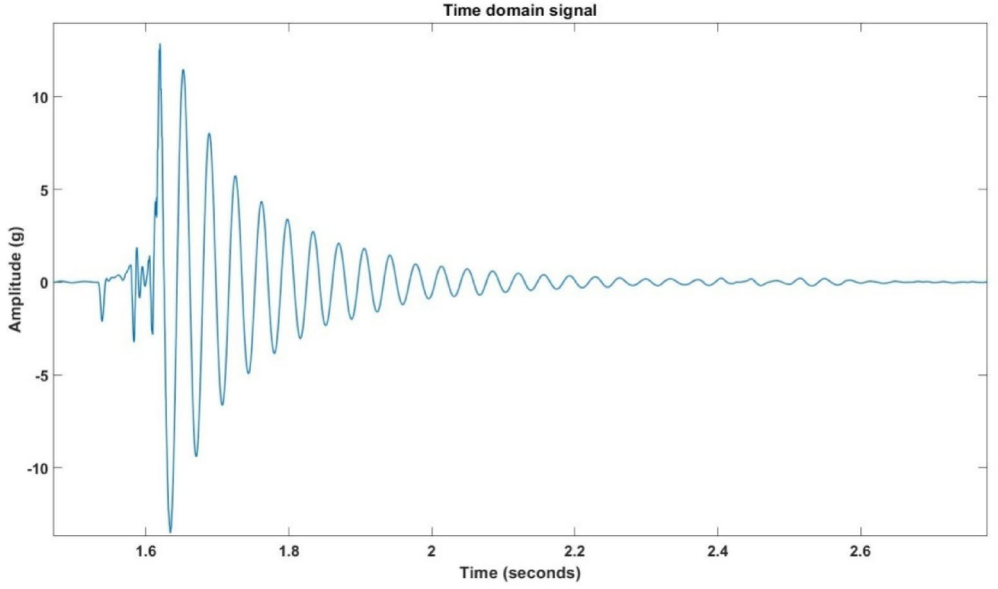

(d)

Fig. 11. (continued)

Conclusions

The domain of sisal fiber-reinforced polyester composites exhibits considerable potential, and this study emphasizes the importance of optimizing fiber concentration to balance strength, dynamic behaviour, and thermal stability.

- The research investigation indicates that both 15% and 20% of sisal fibers yield good results, through the analysis, 15% sisal fiber content optimally performs better than 20% of sisal fiber.
- Shear strength improved significantly, showing a 67.8% increase when the fiber content increased from 5% to 15%, and compressive strength continued to improve up to a 20% fiber concentration. Impact resistance reached its maximum at 16 J with 20% fiber content, demonstrating the relationship between fiber loading and performance.

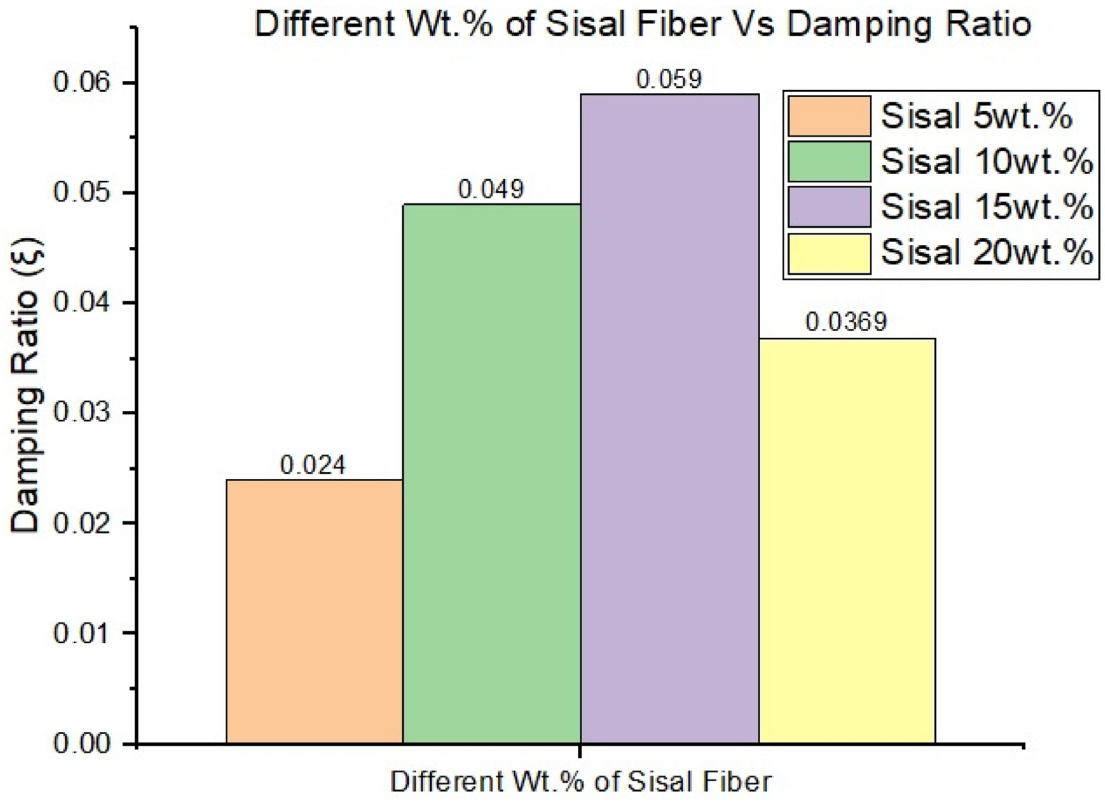

Fig. 12. Wt. of sisal fiber vs. damping ratio.

Sl. no.	Sample	Time (sec)
1	Sisal 5%	3.8
2	Sisal 10%	3.3
3	Sisal 15%	2.4
4	Sisal 20%	2.8

Table 5. Decay time.

- The 15% sisal fiber content performs significantly better than 20%; the shear strength is 41% higher, the flexural strength is 34% higher, and the tensile strength is 47% higher, indicating superior performance in 60% of mechanical properties.
- Thermal analysis showed complete mass retention up to 300 °C, followed by rapid decomposition at 400 °C, with heat flux peaks at 600 °C. SEM imaging revealed that the distribution and orientation of fibers significantly influence mechanical properties.
- The 15% sisal fiber-based composite material is most suitable for the structural applications because it yields a better tensile strength of 17.44 MPa, flexural strength of 52.65 MPa, and shear strength of 77.97 MPa. These properties are good for beams, panels, and structural parts requiring bending resistance and load transfer. While 20% performs better in impact absorption, this characteristic is less crucial for most structural uses, making 15% the better choice for construction and structural components.
- Based on the comprehensive analysis, it is strongly recommended that the developed composite with 15% sisal fiber reinforcement be utilized in the fabrication of lightweight, semi-structural components such as interior automotive panels, partitioning boards, false ceilings, and furniture, where a superior balance of tensile, flexural, and shear strength is paramount, and the operational temperature remains below its degradation threshold of 300 °C.
- Furthermore, the investigation revealed that augmenting sisal fiber content beyond a certain optimal threshold (15%) adversely influences the characteristics of the composite material. An increase to 20% fiber content resulted in insufficient dispersion, fiber clustering, and a decline in tensile, flexural, and shear strengths. Elevated fiber content further diminished the damping factor at increased frequencies and temperatures.

The principal constraints of the study concerning sisal fiber-reinforced polyester composites pertain to the fabrication methodology and the constituent materials. The hand lay-up technique and the application of

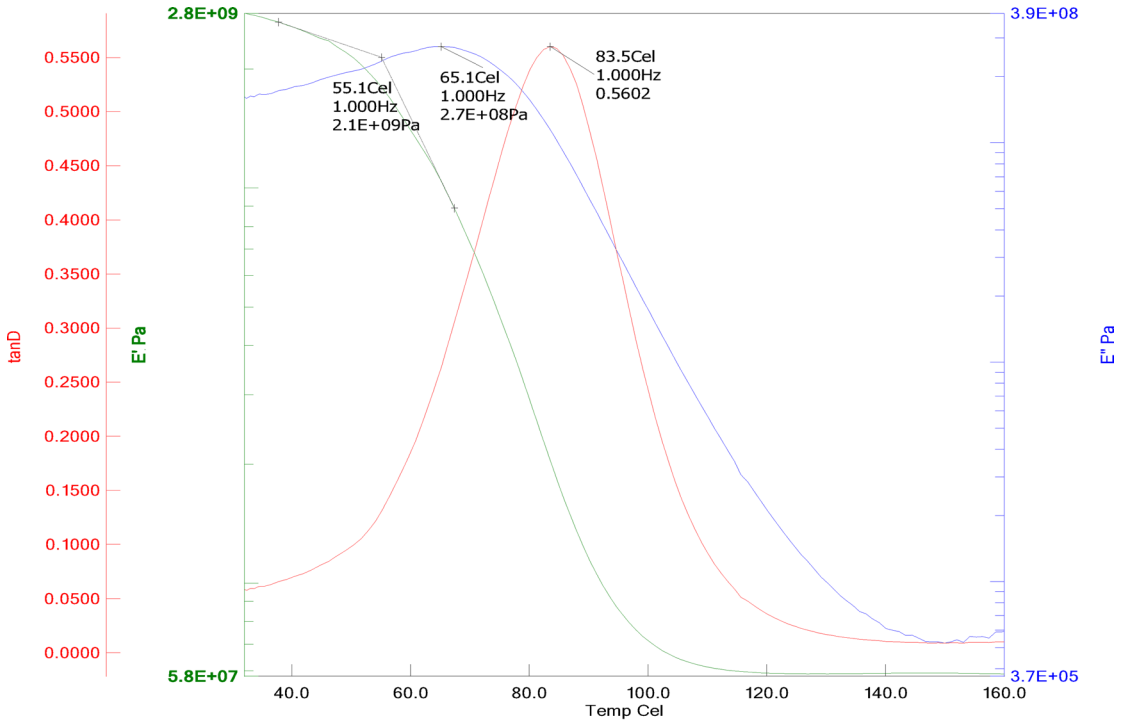

(a)

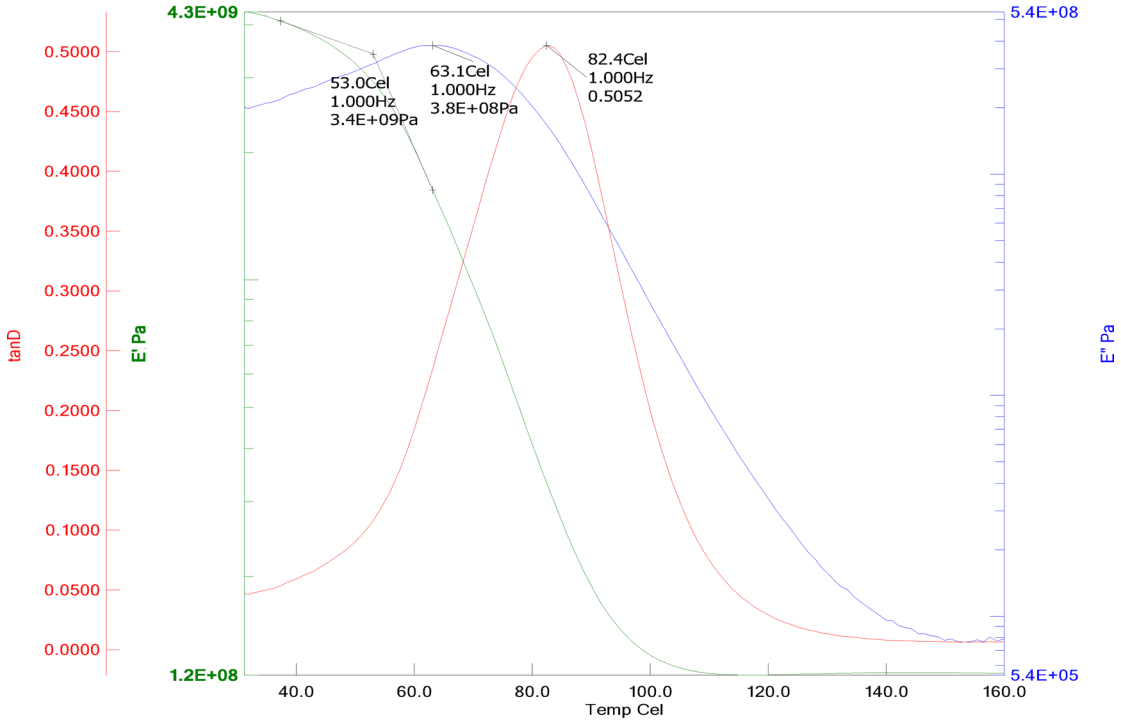

(b)

Fig. 13. (**a**) Viscous-elastic analysis of 5 Wt.% of sisal fiber; (**b**) Viscous-elastic analysis of 10 Wt.% of sisal fiber; (**c**) Viscous-elastic analysis of 15 Wt.% of sisal fiber; (**d**) Viscous-elastic analysis of 20 Wt.% of sisal fiber.

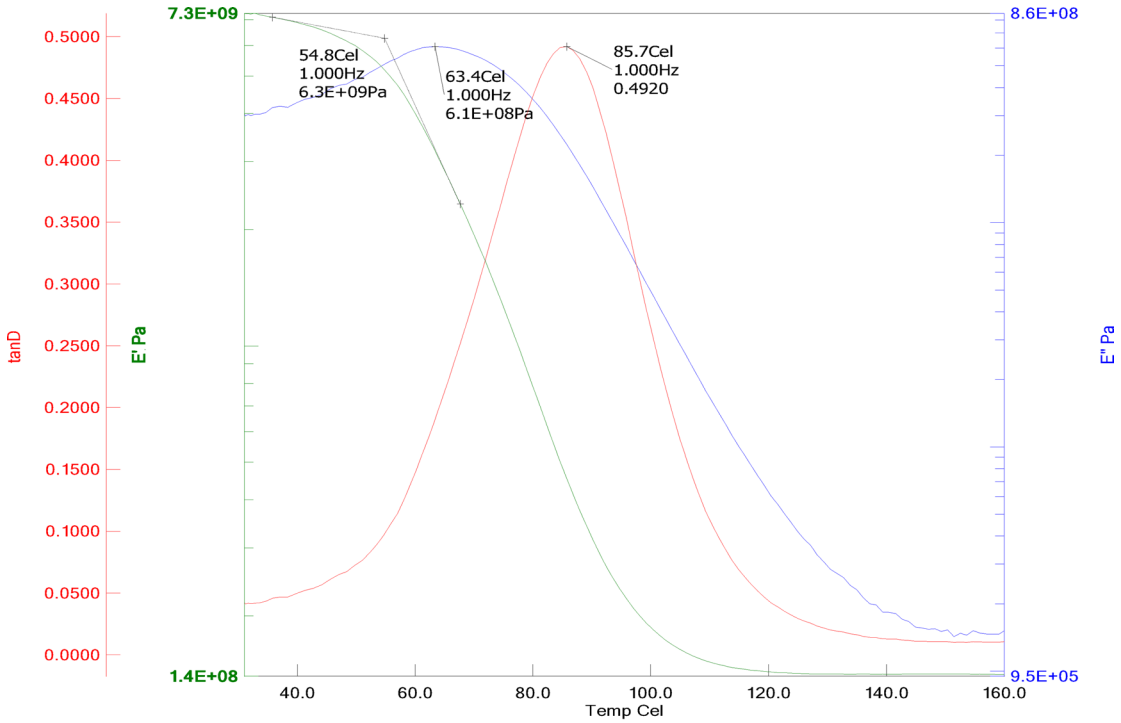

(c)

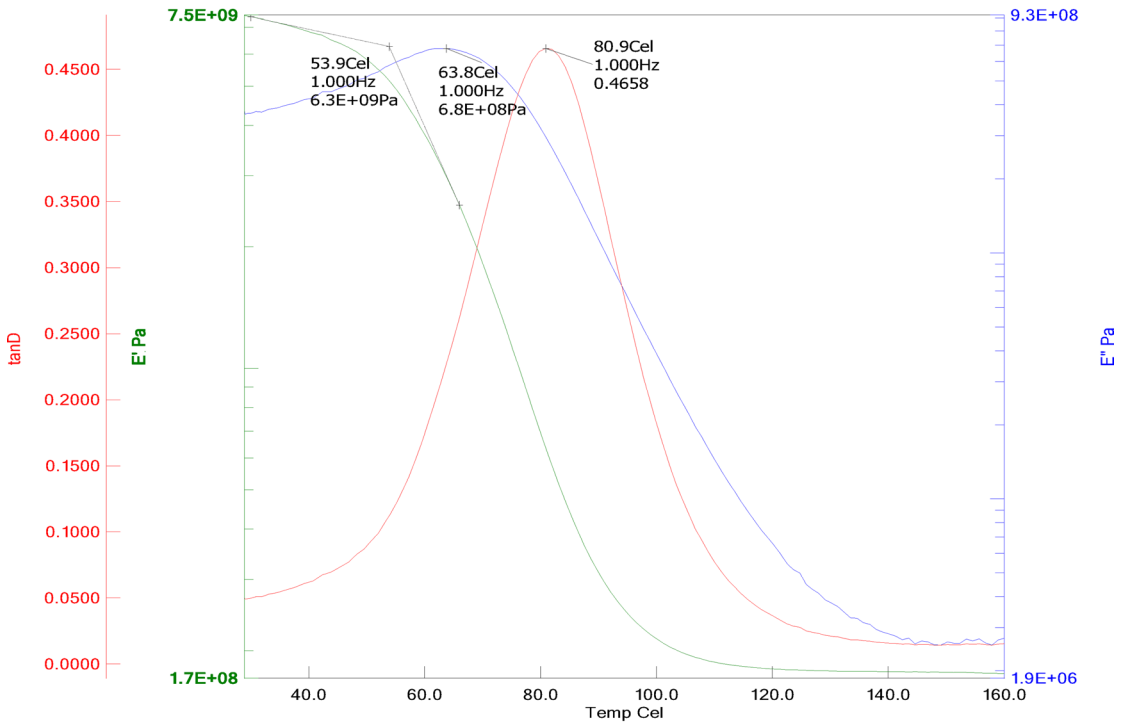

(d)

Fig. 13. (continued)

polyester resins have intrinsic limitations, including prolonged production times, challenges in achieving high fiber-to-resin ratios, as well as the resin's inadequate adhesion properties and high-water permeability.

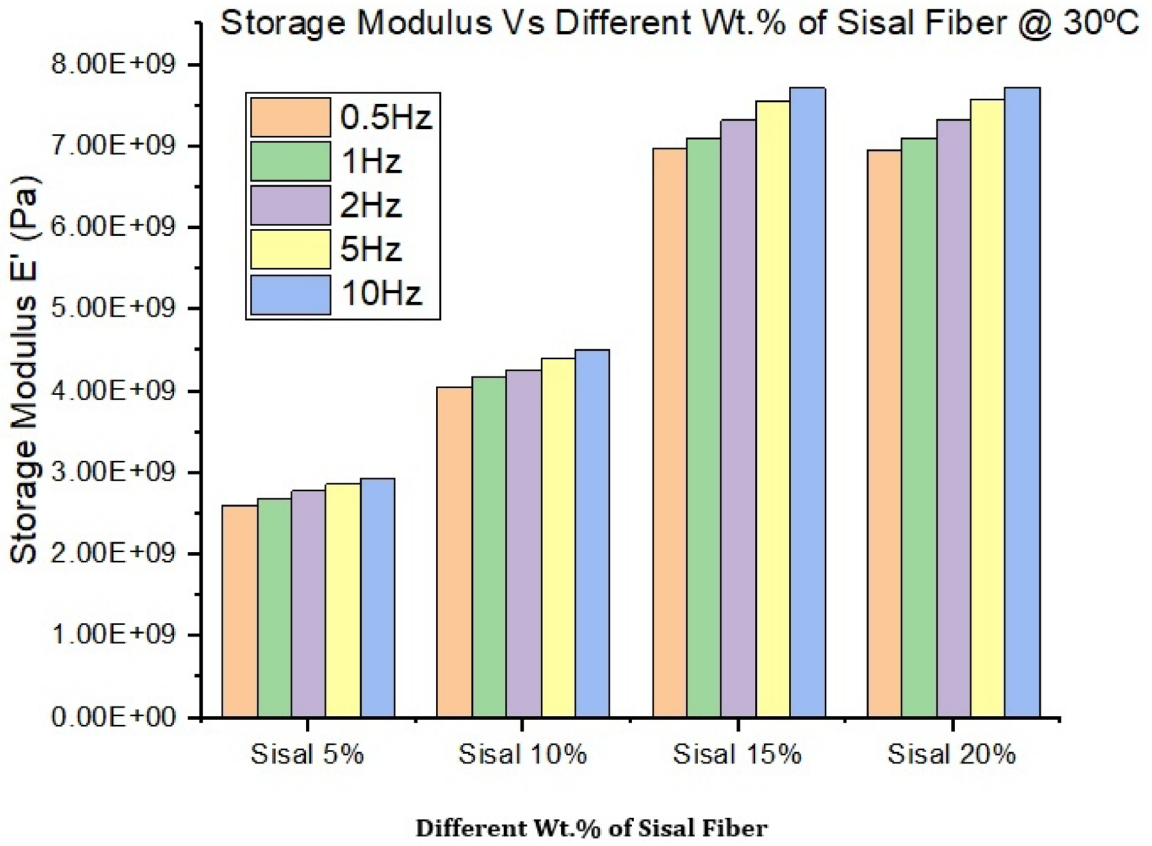

Fig. 14. Storage modulus vs. varying frequency with constant thermal level.

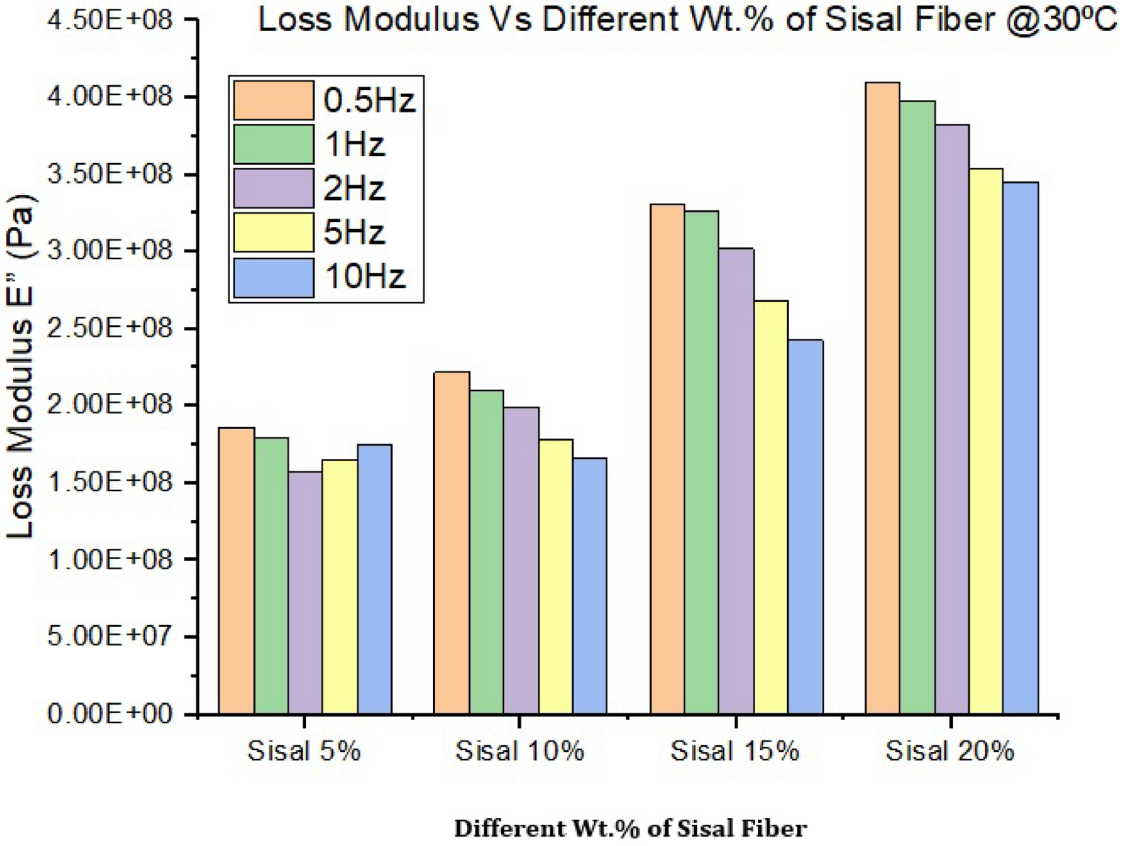

Fig. 15. Viscous modulus vs. varying frequency & materials with constant thermal level.

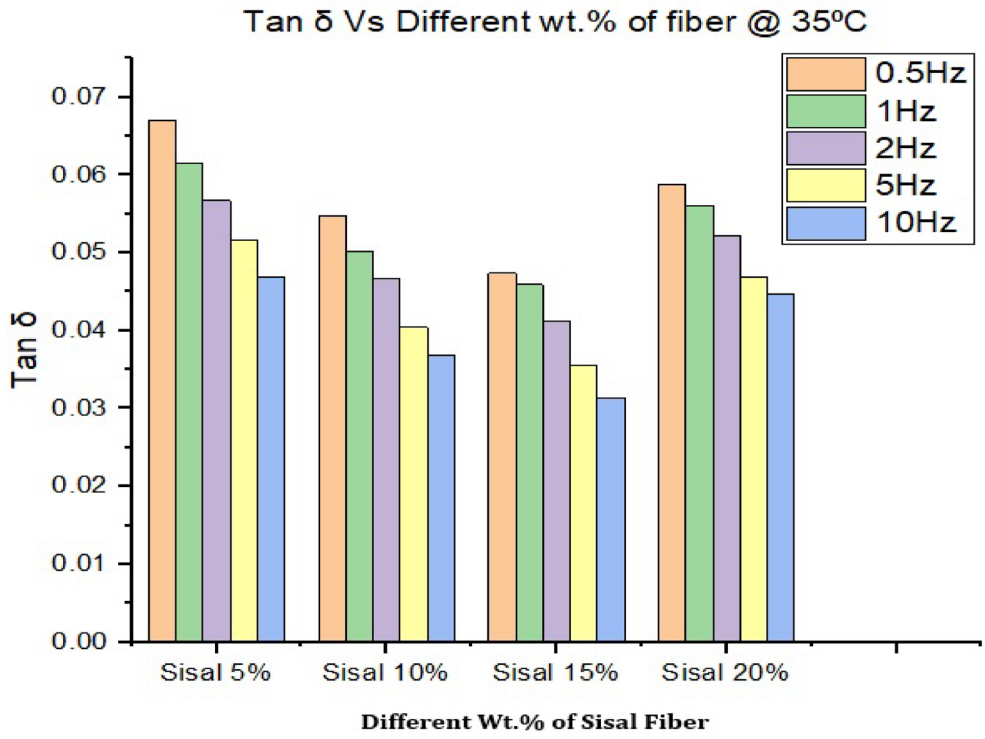

Fig. 16. Loss factor vs different wt% of fiber with constant thermal level varying frequency.

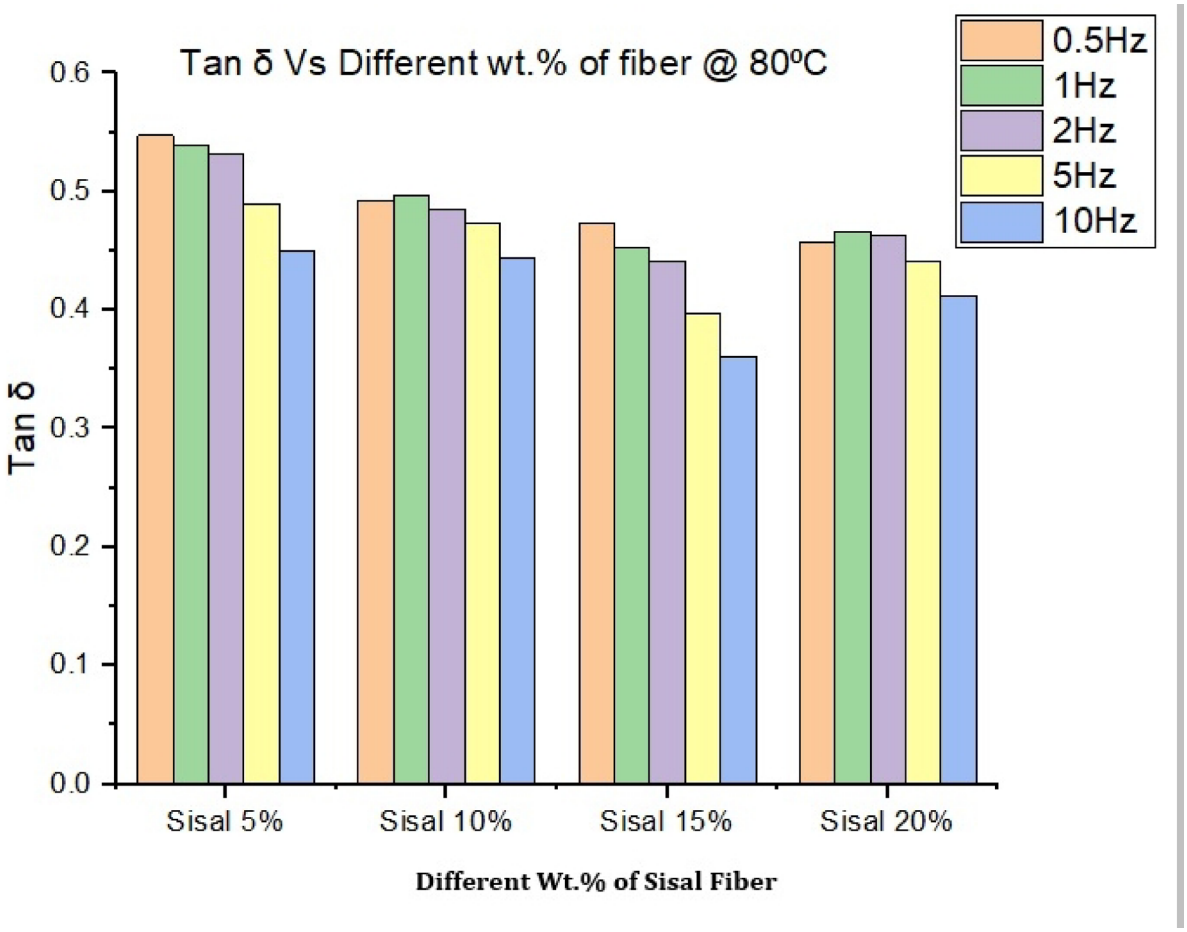

Fig. 17. Loss factor vs varying frequency & materials with constant thermal level.

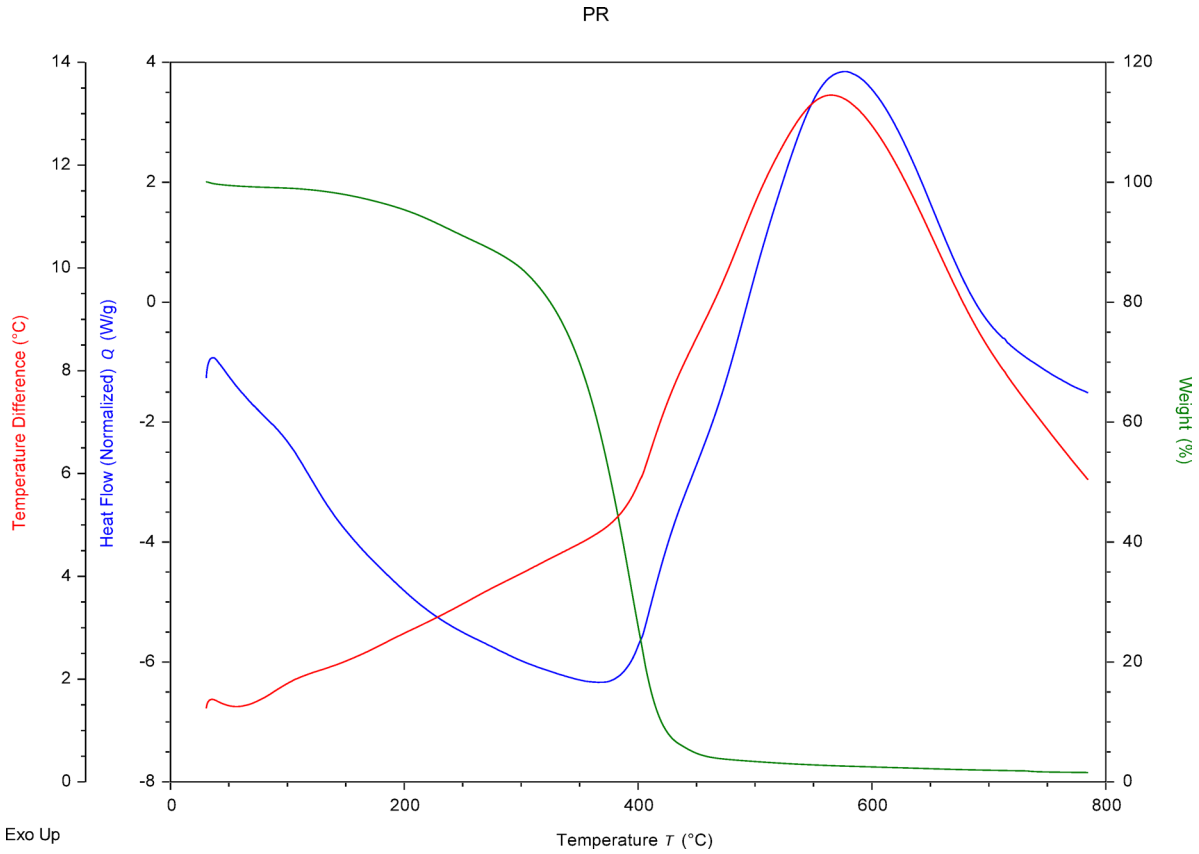

Fig. 18. Thermal analysis of 15 Wt.% of sisal fiber.

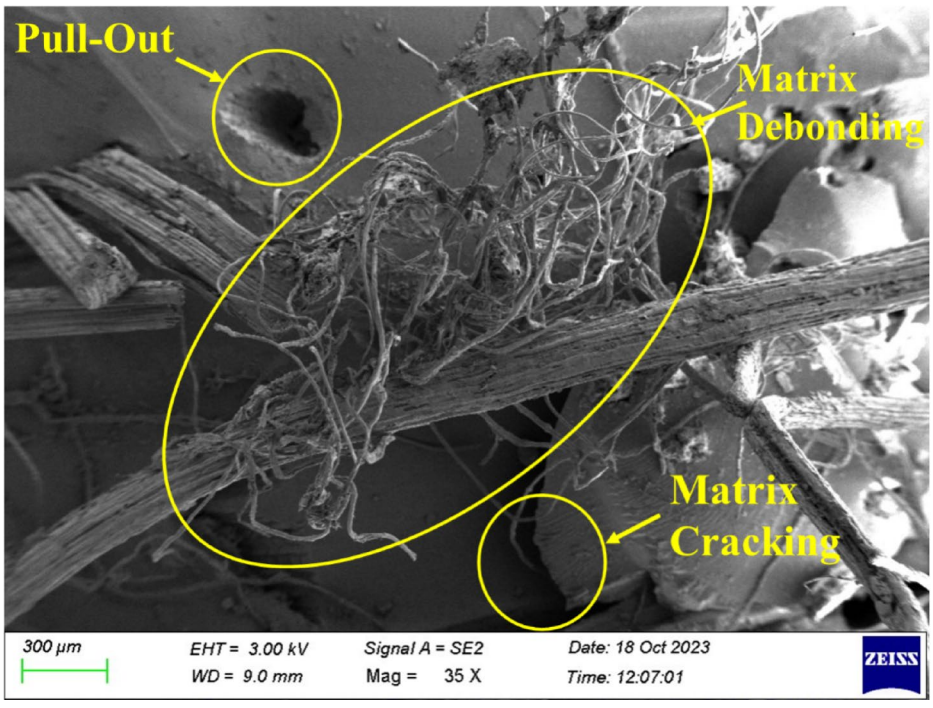

Fig. 19. SEM image of 5% sisal fiber composite material.

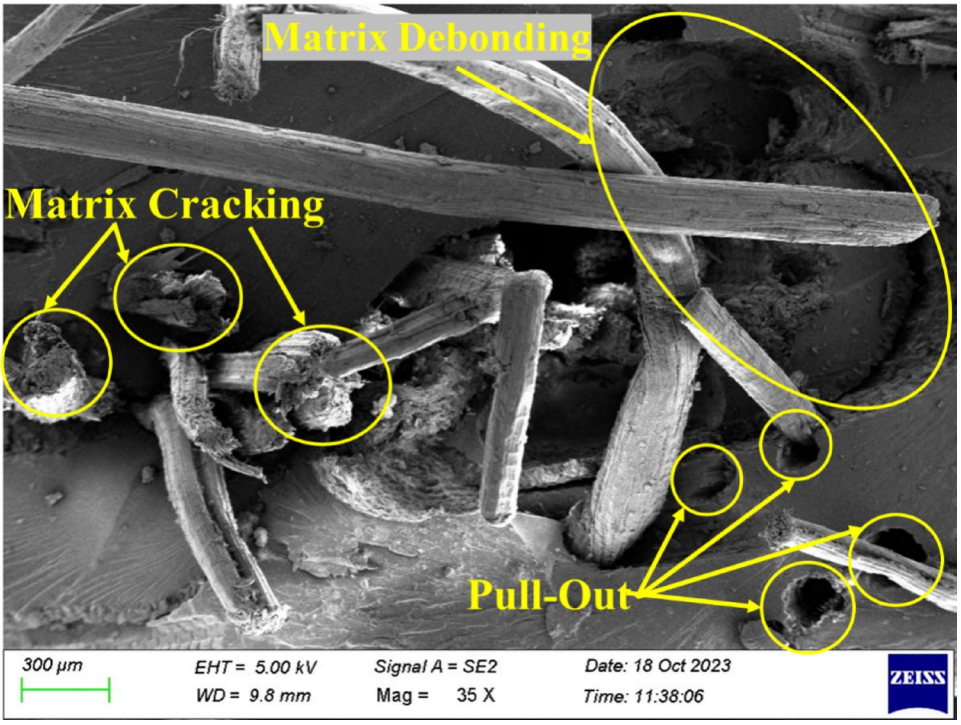

Fig. 20. SEM image of 10% sisal fiber composite material.

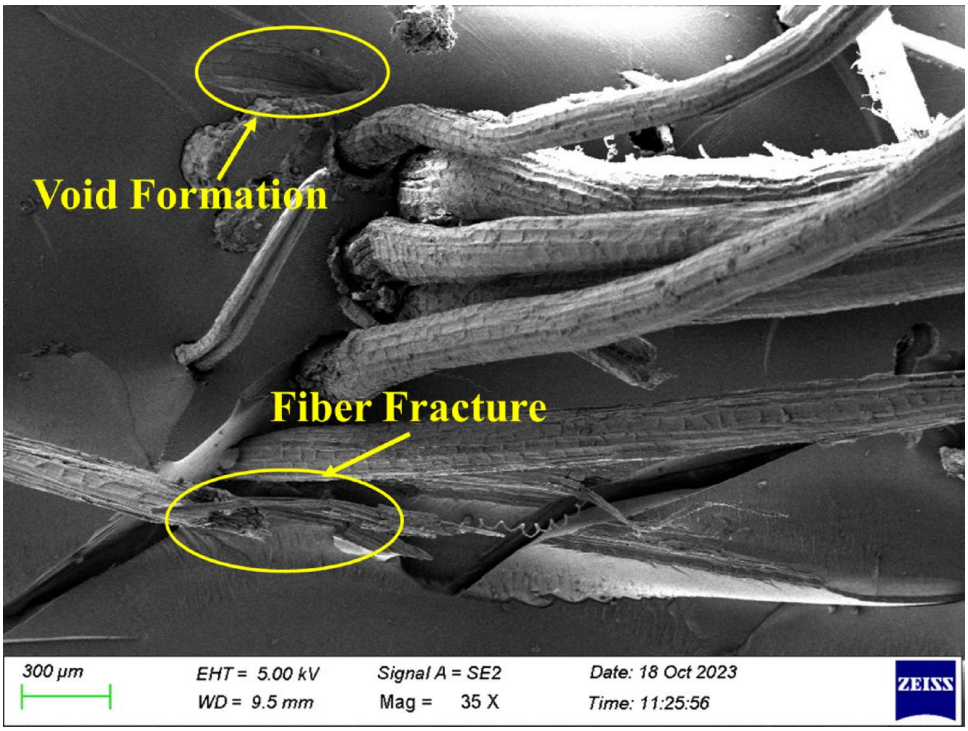

Fig. 21. SEM image of 15% sisal fiber composite material.

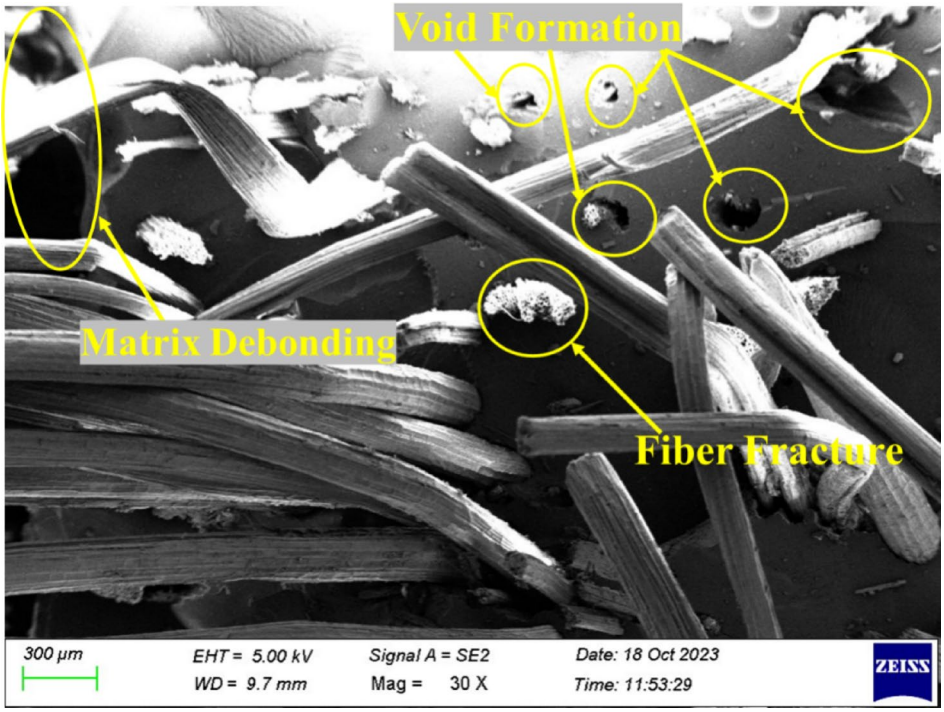

Fig. 22. SEM image of 20% sisal fiber composite material.

Data availability

The datasets generated during and/or analyzed during the current study are available from the corresponding author on reasonable request.

Received: 18 June 2025; Accepted: 12 September 2025
Published online: 17 October 2025

References

1. Etaati, A., Mehdizadeh, S. A., Wang, H. & Pather, S. Vibration damping characteristics of short hemp fibre thermoplastic composites. *J. Reinf Plast. Compos.* **33**, 330–341 (2014).
2. Balasubramanian, R. et al. Synthesis of porous biocarbon from Artocarpus hirsutus husks and its microwave shielding effect on Agave Fiber-Reinforced vinyl ester composite at High-Frequency bands. *Fibers Polym.* **26**, 1281–1296 (2025).
3. Lakshmaiya, N. et al. Development of eco friendly hybrid nanocomposites with improved antibacterial and mechanical properties through NaOH treated natural fibers. *Results Eng.* https://doi.org/10.1016/j.rineng.2025.104996 (2025).
4. Jawaid, M., Khalil, H. P. S. A., Hassan, A., Dungani, R. & Hadiyane, A. Effect of jute fibre loading on tensile and dynamic mechanical properties of oil palm epoxy composites. *Compos. Part. B Eng.* **45**, 619–624 (2013).
5. Balguri, P. K. et al. Characterization of vinyl silane–treated Areca nut woven fiber and bronze filler toughened polyester composite. *Biomass Convers. Biorefinery*. **15**, 14429–14439 (2025).
6. SathishKumar, G., Sridhar, R., Sivabalan, S. & Pugazhenthi, R. Dynamic analysis of the natural fiber (Coir) reinforce polyester composite material with mechanical properties. *Mater. Today Proc.* **69**, 1292–1299 (2022).
7. Rajini, N., Jappes, J. T. W., Rajakarunakaran, S. & Jeyaraj, P. Mechanical and free vibration properties of montmorillonite clay dispersed with naturally woven coconut sheath composite. *J. Reinf Plast. Compos.* **31**, 1364–1376 (2012).
8. Berthelot, J-M. Damping analysis of orthotropic composites with interleaved viscoelastic layers: modeling. *J. Compos. Mater.* **40**, 1889–1909 (2006).
9. Khanna, R., Sharma, N., Kumar, N., Gupta, R. D. & Sharma, A. WEDM of al/sic/ti composite: A hybrid approach of RSM-ARAS-TLBO algorithm. *Int. J. Light Mater. Manuf.* **5**, 315–325 (2022).
10. Romanzini, D., Ornaghi, H. L. Jr, Amico, S. C. & Zattera, A. J. Influence of fiber hybridization on the dynamic mechanical properties of glass/ramie fiber-reinforced polyester composites. *J. Reinf Plast. Compos.* **31**, 1652–1661 (2012).
11. Sharma, N., Sharma, V. S., Sharma, R. C., Arora, R. & Sharma, A. Development of quality microholes by electrical discharge drilling on al/sic composite using of Grey-desirability approach. *Int. J. Light Mater. Manuf.* **5**, 267–277 (2022).
12. Venkateshwaran, N., ElayaPerumal, A. & Jagatheeshwaran, M. S. Effect of fiber length and fiber content on mechanical properties of banana fiber/epoxy composite. *J. Reinf Plast. Compos.* **30**, 1621–1627 (2011).
13. Rajini, N., Jappes, J. T. W., Rajakarunakaran, S. & Jeyaraj, P. Dynamic mechanical analysis and free vibration behavior in chemical modifications of coconut sheath/nano-clay reinforced hybrid polyester composite. *J. Compos. Mater.* **47**, 3105–3121 (2013).
14. Kaushik, V. et al. Influence of cow Dung Ash and TiB2 on the physicomechanical and tribological performance of Al6061-based hybrid composites. *Results Eng.* **19**, 101311 (2023).
15. Saha, A., Kumar, S. & Kumar, A. Influence of pineapple leaf particulate on mechanical, thermal and biodegradation characteristics of pineapple leaf fiber reinforced polymer composite. *J. Polym. Res.* **28**, 66 (2021).
16. Saha, A., Kulkarni, N. D. & Kumari, P. Development of Bambusa tulda-reinforced different biopolymer matrix green composites and MCDM-based sustainable material selection for automobile applications. *Environ. Dev. Sustain.* **27**, 10655–10691 (2025).
17. Kumar, S., Saha, A. & Zindani, D. Agro-waste-based polymeric composite laminates for aerospace cabin interior and identification of their optimal configuration. *Biomass Convers. Biorefinery*. **14**, 31907–31923 (2024).

18. Kumar, S. & Saha, A. Utilization of coconut shell biomass residue to develop sustainable biocomposites and characterize the physical, mechanical, thermal, and water absorption properties. *Biomass Convers. Biorefinery*. **14**, 12815–12831 (2024).
19. Sathish Kumar, G. et al. Mechanical and dynamic properties of banana Fiber-Reinforced polyester composites: A Multi-Analytical characterization study. *Eng. Rep.* **7**, e70200 (2025).
20. Raja, T. et al. Studies on mechanical and morphological behaviors of banyan/kevlar fibers reinforced MgO particulates hybrid aliphatic epoxy composite. *Int. J. Adv. Manuf. Technol.* **2023**:1–8 .
21. Thandavamoorthy, R. et al. Evaluation of mechanical and water absorption properties of kevlar/carbon/basalt fibers reinforced nano cellulose particulates Bisphenol-F LY556 epoxy composite. *Int. J. Adv. Manuf. Technol.* https://doi.org/10.1007/s00170-023-12152-z (2023).
22. SathishKumar, G. et al. Investigation of mechanical properties, viscoelastic properties and free vibration analysis of natural fibre reinforced composite materials. *Interactions* **245**, 321 (2024).
23. Antony, A. G., Vijayan, V., Saravanan, S., Baskar, S. & Loganathan, M. Analysis of wear behaviour of aluminium composite with silicon carbide and titanium reinforcement. *Int. J. Mech. Eng. Technol.* **9**, 681–691 (2018).
24. Tengsuthiwat, J. et al. Lignocellulose sustainable composites from agro-waste asparagus bean stem fiber for polymer casting applications: effect of fiber treatment. *Int. J. Biol. Macromol.* **278**, 134884 (2024).
25. Tengsuthiwat, J., Vinod, A., Vijay, R., Rangappa, S. M. & Siengchin, S. Characterization of novel natural cellulose fiber from Ficus macrocarpa bark for lightweight structural composite application and its effect on chemical treatment. *Heliyon* **10**, e30442 (2024).
26. Raghunathan, V. et al. *Sustainable Characterization of Brake Pads Using raw/silane-treated Mimosa Pudica Fibers for Automobile Applications* (Polym Compos, 2024).
27. Raghunathan, V., Ayyappan, V., Rangappa, S. M. & Siengchin, S. Development of fiber-reinforced polylactic acid filaments using untreated/silane-treated trichosanthes cucumerina fibers for additive manufacturing. *J. Elastomers Plast.* **56**, 277–292 (2024).
28. Vinod, A., Tengsuthiwat, J., Vijay, R., Sanjay, M. R. & Siengchin, S. Advancing additive manufacturing: 3D-printing of hybrid natural fiber sandwich (Nona/soy-PLA) composites through filament extrusion and its effect on thermomechanical properties. *Polym. Compos.* **45**, 7767–7789 (2024).
29. Devarajan, B. et al. Recent developments in natural fiber hybrid composites for ballistic applications: a comprehensive review of mechanisms and failure criteria. *Facta Univ. Ser. Mech. Eng.* https://doi.org/10.22190/FUME240216037D (2024).
30. Sharma, N., Singh, G., Sharma, R. C., Sharma, A. & Goyal, K. K. Magnesium-based nanocomposites: an overview of applications and challenges. *Powder Metall. Met. Ceram.* **61**, 205–220 (2022).
31. Sathish, M., Radhika, N., Venuvanka, N. & Rajeshkumar, L. A review on sustainable properties of plant fiber-reinforced polymer composites: characteristics and properties. *Polym. Int.* **73**, 887–943 (2024).
32. Shen, Y. et al. High-performance Basalt-fiber-reinforced laminated composites: free of fiber surface modification and sizing agent. *ACS Sustain. Chem. Eng.* **12**, 3863–3875 (2024).
33. Painkal, S. K., Balachandran, M., Jayanarayanan, K., Sridhar, N. & Kumar, S. Synergistic enhancement in mechanical properties of graphene/mwcnt reinforced polyaryletherketone–carbon fiber multi-scale composites: experimental studies and finite element analysis. *Adv. Ind. Eng. Polym. Res.* **8**, 20–36 (2025).
34. Nikhil, K. V. et al. Experimental investigation on vibration characteristics and damping factor of Coir fiber reinforced polyester composite material. *Discov Appl. Sci.* **7**, 465 (2025).
35. Sathishkumar, T. P. et al. Effects of cashew nutshell biofillers on the mechanical and thermal behaviour of basalt/hibiscus vitifolius hybrid fabrics reinforced polymer biocomposites. *Sci. Rep.* **14**, 27636 (2024).
36. Faisal, N. et al. *Experimental Analysis for the Performance Assessment and Characteristics of Enhanced Magnesium Composites Reinforced with Nano-Sized Silicon Carbide Developed Using Powder Metallurgy* (ACS Omega, 2024).
37. Senthil Kumar, M. S., Rajeshkumar, L., Rangappa, S. M. & Siengchin, S. Mechanical behaviour analysis for banana/coir natural fiber hybrid epoxy composites through experimental modelling. *J. Polym. Res.* **31**, 163 (2024).
38. Ramesh, M., Rajeshkumar, L., Sanjay, M. R. & Siengchin, S. Sustainable biocomposites based on polylactic acid and agro waste biofillers for lightweight applications: Fabrication and properties. *J. Thermoplast Compos. Mater.* https://doi.org/10.1177/08927057251322165 (2025).
39. Sugözü, B., Erol, E. & Sugözü, İ. Tribological and thermal characteristics of copper-free brake friction composites. *Mater. Test.* **66**, 226–232 (2024).
40. Sugözü, B., Dağhan, B., Akdemir, A. & Sugözü, İ. Effect of micro and nano-sized ZrSiO4 particles on the friction and wear properties of polymer matrix composites. *Mater. Test.* **64**, 1290–1297 (2022).

Author contributions

G. Sathish Kumar : Writing-original draft Uma Devi A. : Investigation M. Prem Kumar Reddy : Conceptualization Vishvanath N. Kanthe : Formal analysis D. Palaniswamy : MethodologyP. R. Kalyana Chakravarthy : Resources M. Dubey : Writing- review & editingHimadri Majumder : Writing- review & editingAshish Kumar Srivastava : Supervision.

Funding

Open access funding provided by Manipal University Jaipur.

Declarations

Competing interests

The authors declare no competing interests.

Software used

OriginPro 2024b (OriginLab Corporation, https://www.originlab.com/) – used for plotting graphs and performing regression analysis.

Additional information

Correspondence and requests for materials should be addressed to A.K.S.